The Cimmerian evolution of the Nakhlak Anarak area, Central Iran, and its bearing for the reconstruction of the history of the Eurasian margin

Andrea Zanchi, Stefano Zanchetta, Eduardo Garzanti, Marco Balini, Fabrizio Berra, Massimo Mattei and Giovanni Muttoni

Geological Society, London, Special Publications 2009; v. 312; p. 261-286
doi:10.1144/SP312.13

The Cimmerian evolution of the Nakhlak–Anarak area, Central Iran, and its bearing for the reconstruction of the history of the Eurasian margin

ANDREA ZANCHI[1], STEFANO ZANCHETTA[1], EDUARDO GARZANTI[1], MARCO BALINI[2], FABRIZIO BERRA[2], MASSIMO MATTEI[3] & GIOVANNI MUTTONI[2]

[1]*Dipartimento Scienze Geologiche e Geotecnologie, Università di Milano-Bicocca, Piazza della Scienza 4, Milano, 20126, Italy (e-mail: andrea.zanchi@unimib.it)*

[2]*Dipartimento di Scienze della Terra, Università di Milano, Via Mangiagalli 34, 20133 Milano, Italy*

[3]*Dipartimento di Scienze Geologiche, Università Roma TRE, Largo San Leonardo Murialdo 1, 00146 Roma, Italy*

Abstract: New structural, sedimentological, petrological and palaeomagnetic data collected in the region of Nakhlak–Anarak provide important constraints on the Cimmerian evolution of Central Iran. The Olenekian–Upper Ladinian succession of Nakhlak was deposited in a forearc setting, and records the exhumation and erosion of an orogenic wedge, possibly located in the present-day Anarak region. The Triassic succession was deformed after Ladinian times and shows south-vergent folds and thrusts unconformably covered by Upper Cretaceous limestones following the Late Jurassic Neo-Cimmerian deformation. Palaeomagnetic data obtained in the Olenekian succession suggest a palaeoposition of the region close to Eurasia at a latitude around 20°N. In addition, the palaeopoles do not support large anticlockwise rotations around vertical axes for central Iran with respect to Eurasia since the Middle Triassic, as previously suggested.

The Anarak Metamorphic Complex (AMC) includes blueschist-facies metabasites associated with discontinuous slivers of serpentinized ultramafic rocks and Carboniferous greenschist-facies 'Variscan' metamorphic rocks, including widespread metacarbonates. The AMC was formed, at least partially, in the Triassic. Its erosion is recorded by the Middle Triassic Bāqoroq Formation at Nakhlak, which consists of conglomerates and sandstones rich in metamorphic detritus. The AMC was repeatedly deformed during post-Triassic times, giving origin to a complex structural setting characterized by strong tectonic fragmentation of previously formed tectonic units.

Based on these data, we suggest that the Nakhlak–Anarak units represent an arc–trench system developed during the Eo-Cimmerian orogenic cycle. Different tectonic scenarios that can account for the evolution of the region and for the occurrence of this orogenic wedge in its present position within Central Iran are critically discussed, as well as its relationships with a presumed 'Variscan' metamorphic event.

The Cimmerian orogeny, affecting the southern Eurasian margin between Turkey and Thailand, is related to the collision of several microplates, most of which detached from northern Gondwana in the Early Permian during the opening of the Neotethys Ocean (Sengör 1979; Stampfli *et al.* 1991; Dercourt *et al.* 2000; Stampfli & Borel 2002; Brunet *et al.* 2003; Torsvik & Cocks 2004; Angiolini *et al.* 2007). The Cimmerian mountain-building event, resulting in the closure of the various branches of the Palaeotethys Ocean, is well documented along the northern margin of Iran, which has always been considered as one of the main Cimmerian blocks. Several authors located the main Palaeotethys suture (Alavi 1991; Boulin 1991; Ruttner 1993) in the region around Mashhad, as first suggested by Stöcklin (1974). More recent reconstructions (Alavi 1991; Ruttner 1993; Alavi *et al.* 1997) identified an accretionary wedge in this area related to the northward subduction of a Palaeotethyan branch below Eurasia (Fig. 1). The possible continuation of the suture along the northern margin of the present-day Alborz chain (Alavi 1996) has been discussed in several papers (Zanchi *et al.* 2006, 2009; Berra *et al.* 2007) that also suggest the occurrence of an important 'Variscan' *sensu latu* tectono-metamorphic event in the allochthonous nappes emplaced on the northern margin of Iran during the Eo-Cimmerian collision (Zanchetta *et al.* 2009).

From: BRUNET, M.-F., WILMSEN, M. & GRANATH, J. W. (eds) *South Caspian to Central Iran Basins*. The Geological Society, London, Special Publications, **312**, 261–286.
DOI: 10.1144/SP312.13 0305-8719/09/$15.00

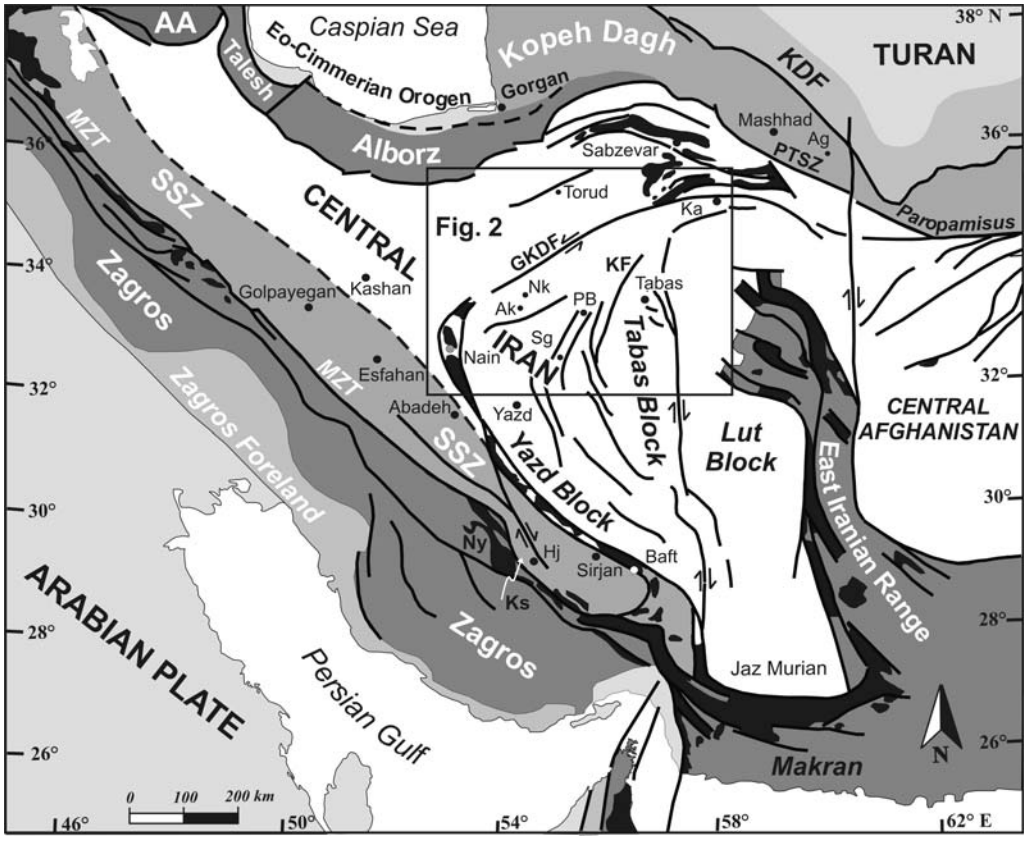

Fig. 1. Tectonic scheme of Iran with the main tectonic subdivisions. White, Cimmerian blocks; black, Mesozoic ophiolites along the Main Zagros and other sutures; modified from Angiolini *et al.* (2007). AA, Araxian–Azarbaijanian Zone; Ag, Aghdarband Basin; Ak, Anarak; GKDF, Great Kavir–Doruneh fault system; Hj, Hajiabad metamorphic complex; KDF, Kopeh Dagh Foredeep; KF, Kalmard Fault; Ks, Kor-e-Sefid metamorphic complex; MZT, Main Zagros thrust; Nk, Nakhlak Basin; Ny, Neyriz ophiolites; PB, Posht-e Badam; PTSZ, Palaeotethys Suture Zone; Sg, Saghand; SSZ, Sanandaj–Sirjan Zone.

The Palaeotethys collision zone is also exposed eastward along the Paropamisus and Northern Pamir ranges (Boulin 1988, 1991).

The Gondwanan affinity of the blocks forming Iran is supported by several lines of evidence (Stöcklin 1974; Berberian & King 1981), based on the similarity of their late Proterozoic 'Pan-African' basement, the affinity of the late Pre-Cambrian and Cambrian successions across the Zagros suture, and the lack of a 'Variscan' deformation (Saidi *et al.* 1997).

The Gondwanan affinity of Iran is also demonstrated by U–Pb geochronological data on granitoids belonging to the crystalline basement of Sanandaj–Sirjan, central Iran and the Alborz Mountains, which have given late Neoproterozoic–Early Cambrian ages (Hassanzadeh *et al.* 2008). Their presence in Iran is explained by the development of an active continental margin in the Peri-Gondwana region at the end of the Neoproterozoic, as also suggested by the geochemical affinity of these rocks (Ramezani & Tucker 2003).

The final collision of the Iranian composite plate with Eurasia occurred during the Late Triassic, and is marked by a regional unconformity sealed by the deposition of the Upper Triassic–Jurassic Shemshak Group (Fürsich *et al.* 2009; Zanchi *et al.* 2009). U–Pb zircon ages of 220–210 Ma (Horton *et al.* 2008) from this clastic succession provide control on the time of the collision.

Other authors (Boulin 1988, 1991; Golonka 2004) proposed a different scenario, hypothesizing that Iran was composed of different microplates (Alborz–north Iran and central Iran–Lut) that detached from Gondwana at different times and progressively collided with the composite southern Eurasian active margin during the Mesozoic.

The Nakhlak–Anarak region, located in the middle part of central Iran south of the Great Kavir Fault (Fig. 1), is thus a key area in understanding the Late Palaeozoic–Triassic evolution of Iran. In fact, the peculiar arc-related Triassic succession of Nakhlak shows contrasting features with the dominant carbonate platform facies widespread from the Alborz Mountains to the northern margin of the Jaz Murian depression (Alavi *et al.* 1997; Seyed-Emami 2003). The Olenekian–Ladinian succession consists of pelagic sedimentary rocks including *Rosso ammonitico* facies, volcanic arenites, alluvial fan conglomerates and turbidites deposited in a volcanic arc setting along an active margin (Balini *et al.* 2009). A few kilometres to the south of Nakhlak, the Anarak Metamorphic Complex (AMC) is exposed. It consists of an intricate rock association including metapelites, metabasites and marbles associated with slivers of ultramafic rocks (Sharkovski *et al.* 1984), interpreted as an accretionary wedge active from Late Palaeozoic–Triassic times (Bagheri & Stampfli 2008). The AMC is sharply interrupted westward by the Upper Cretaceous 'Coloured Mélange', forming a more recent ophiolitic 'ring' that surrounds the internal portion of central Iran.

The occurrence of this peculiar rock association within continental Iran poses several questions regarding its evolution and especially on the number of Cimmerian (Palaeotethys) sutures (single rather than multiple) between Eurasia and Iran (Stöcklin 1974; Sengör 1979, 1990; Berberian & King 1981; Alavi 1991; Stampfli & Borel 2002; Bagheri & Stampfli 2008). Previous authors (Davoudzadeh & Weber-Diefenbach 1987; Soffel *et al.* 1996; Alavi *et al.* 1997) explained the anomalous position of the Nakhlak–Anarak region in terms of sparse palaeomagnetic data that apparently showed a post-Triassic 135° anti-clockwise rotation of central Iran. That rotation was supposed to be responsible for displacing a large fragment of the Palaeotethys suture from the present-day Afghan–Iranian border region. However, new palaeomagnetic information obtained from the Olenekian succession of Nakhlak (Muttoni *et al.* 2009) challenges that interpretation and suggests that no large rotations have occurred in the area since the Triassic.

In this paper, we describe the structural setting of the Nakhlak–Anarak region and outline aspects of the evolution of the region that remain problematic.

How many blocks form Iran?

A basic problem in the literature is the definition of the different Late Palaeozoic–Middle Triassic domains that comprised Iran. The idea that Iran consists of more than one block is directly related to its complex setting, chiefly due to the occurrence of several ophiolitic belts that are assumed to record the opening and closure of several oceanic basins, and to the activity of large active intracontinental faults that split the area in several partially independent blocks. The evolution of Iran through time is complex owing to the continuous aggregation and differential motion between several blocks.

According to the first reconstructions presented by Stöcklin (1974) and Berberian & King (1981), three main regions can be recognized during Palaeozoic–Triassic times: North Iran, Central Iran and the Sanandaj–Sirjan Zone. Following Berberian & King (1981) and the main subdivisions adopted in the Geological Survey of Iran's 1:250 000 maps of Iran, north Iran includes the Alborz region, its boundary with central Iran running just to the south of the mountain belt. The Alborz belt is a Late Tertiary intracontinental belt (Allen *et al.* 2003) reactivating a Late Triassic orogen which itself was produced by the collision of Iran with the southern margin of Eurasia (Zanchi *et al.* 2009). The late Precambrian–Triassic succession is very similar to the sequences found in the other regions of Iran and, at least for a large part of the Palaeozoic, shows a Gondwanan affinity (Stöcklin 1974; Berberian & King 1981; Wendt *et al.* 2005; Angiolini *et al.* 2007).

Central Iran occupies the internal part of Iran, and is a very complex and poorly known area, characterized by desert areas with poor exposures. The most peculiar feature is the occurrence of an Upper Mesozoic ophiolitic 'ring', the so-called 'Coloured Mélange', which delimits its most internal part (Figs 1 and 2). Central Iran is also affected by a complex system of active intracontinental strike-slip faults (Fig. 1) causing an intensive north–south dextral shearing of the whole area (Walker & Jackson 2004). The left-lateral Great Kavir–Doruneh fault system to the north, crossing the northern part of central Iran, currently bounds the deformational system to the north. The deformation is accommodated within central Iran by N–S-trending dextral faults, which separate the Yazd, Tabas and Lut blocks. These faults are possibly inherited from Precambrian times (Berberian & King 1981) and were active during the Palaeozoic evolution of the region, as testified by facies and thickness variations across these structures (Wendt *et al.* 2005).

The boundary between North and Central Iran coincides with minor facies changes in the Palaeozoic–Triassic successions. In addition, Leven & Gorgij (2006) and Gaetani *et al.* (2009) show a striking similarity between the Permo-Carboniferous stratigraphic evolution of North and Central Iran, suggesting the absence of biotic barriers and thus their contiguity. Minor differences

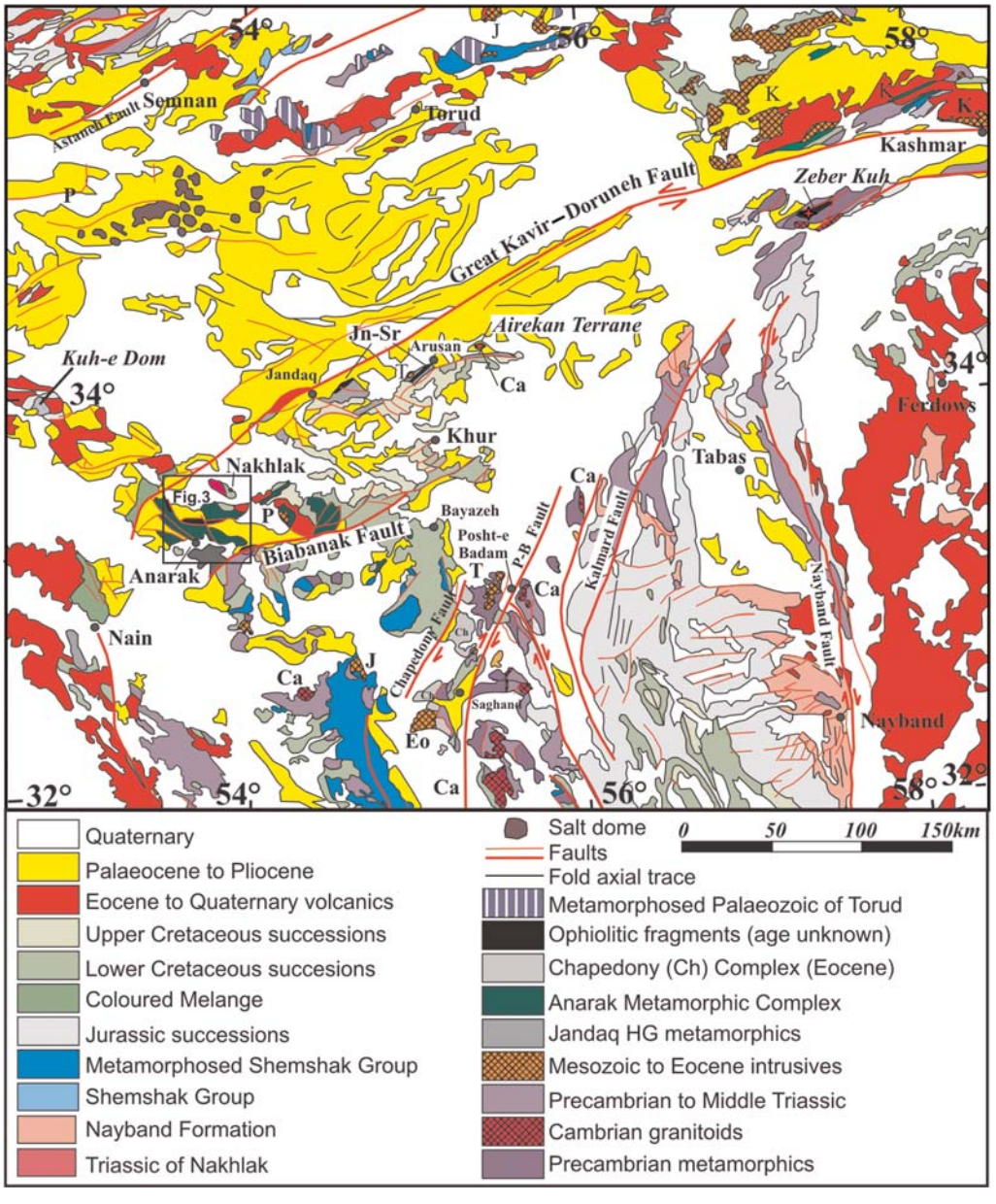

Fig. 2. General structural map of part of Central Iran, obtained from available maps (Geological Survey of Iran 1976, 1977, 1984*a–c*, 1987, 1989; Bagheri & Stampfli 2008) and from Ramezani & Tucker (2003). The square shows the location of Figure 3. Jn-Sr, ZK-Sr, ophiolitic fragments of Jandaq-Arusan and Zeber Kuh; Ch, Chapedony Complex (Eocene). Ca, Cambrian; T, Late Triassic; J, Jurassic; K, Cretaceous; P, Palaeocene; Eo, Eocene refer to radiometric ages of granitoids; P-B, Posht-e-Badam.

occur in the Abadeh region, located along the eastern border of the Sanandaj–Sirjan Zone. North Iran thus represents the northern margin of the Central Iran block at least for the Palaeozoic. The same conclusion is reached by Wendt *et al.* (2002, 2005), who extensively reviewed the Palaeozoic successions of Iran. According to their work, most of the area, with a few exceptions in the Talesh Mountains (see also Zanchi *et al.* 2009 for a discussion) and east of Mashhad (Āghdarband basin), southern

Alborz, as well as the Yazd, Tabas and Lut blocks, belongs to the stable northern margin of Gondwana. No clear separation is evident during most of the Late Palaeozoic. The same authors exclude strongly subsided Devonian basins that were later affected by Variscan orogenic movements ('mobile zones') along the western margin of central Iran and in the southern Sanandaj–Sirjan Zone, as did Davoudzadeh & Weber-Diefenbach (1987). These authors, in fact, recognize the occurrence of isolated blocks within central Iran that were affected by a Variscan metamorphism: the Anarak metamorphic rocks, some of the metamorphic rocks exposed in the Saghand area, which have given a Rb–Sr age of 315 $\pm$ 5 Ma (Crawford 1977), and possibly also the Zeber Kuh beds (Fig. 2) and the Carboniferous phyllites located NE of Tabas and SW of Kashmar. Two hypotheses are discussed by Davoudzadeh & Weber-Diefenbach (1987).

- Occurrence of multiple Palaeotethyan basins separating blocks with different Palaeozoic histories. In their opinion, the Palaeotethys suture located along the northern margin of Iran represents the remnants of the main ocean, whereas a narrow trough was located south of Jaz Murian and the Sanandaj–Sirijan Zone; another trough was located along the Doruneh–Great Kavir fault system and is testified by the occurrence of Variscan metamorphic events.
- The Palaeotethys suture was unique, and metamorphics of the Zeber Kuh–Anarak area were displaced from their original position previously located between Mashhad and Herat during a presumed Meso-Cenozoic anticlockwise rotation of the Central Iran microplate.

Bagheri & Stampfli (2008) document the occurrence of a Late Palaeozoic–Triassic active margin in the area south of the Great Kavir Fault between Anarak and Jandaq, implying a sharp separation between the regions of Central Iran located north and south of this fault. These authors present new palaeontological and Ar–Ar age determinations documenting the evolution of a long-lived active margin between 330 and 230 Ma. They interpret the arc–trench successions as fragments of the Palaeotethys suture zone originally located E–NE of Mashhad and tectonically transported to its present position after the Cimmerian orogeny during the counter-clockwise rotation of central Iran.

A further problem in understanding the structure of Central Iran is caused by the findings of Davidof & Arefifard (2007), who identified cold-water fusulinid assemblages in the Posht-e-Badam area along the Kalmard Fault (Fig. 2), west of Tabas. These are typical cool-water low-diversity peri-Gondwana assemblages, which are distributed from Oman to Karakoram, Central Pamir and the Baoshan block in China. This might indicate that the block lay far south during the Early Permian with respect to North and Central Iran, which show typical warm-water tropical fusulinids (Leven & Gorgij 2006; Angiolini *et al.* 2007).

The Sanandaj–Sirjan Zone (SSZ) is a narrow belt of strongly deformed and metamorphosed rocks sandwiched between the Zagros Orogenic Belt and Central–North Iran (Berberian & King 1981). The SSZ is partially delimited on both sides by supra-subduction ophiolites formed in intra-oceanic island arcs (Ghasemi & Talbot 2006). It mainly consists of Palaeozoic–Mesozoic metamorphic rocks intruded by several generations of Meso-Cenozoic intrusives. Its history culminated in the Eocene Urumieh–Dokhtar magmatic arc that records the main Neotethys slab break-off. Evidence of the origin of the SSZ and of its evolution is controversial, mainly owing to strong tectonic disturbance and metamorphism that often hampers the recognition and dating of the protoliths. A major branch of the Permian Neotethys oceanic basin separated the SSZ block from the present-day Zagros region, which consists of deformed sedimentary rocks entirely belonging to the Arabian margin.

Some authors (Stöcklin 1974; Berberian & King 1981; Ghasemi & Talbot 2006) interpret the SSZ as a block lying along the southern margin of Iran. Recent stratigraphic studies by Wendt *et al.* (2005) south of Kashan indicate that the SSZ was part of Central Iran during the Palaeozoic, showing very similar stratigraphic units. Recent data concerning the study of the protoliths of the Mesozoic metamorphic rocks exposed in the Muteh area, NW of Isfahan, also suggest that they represent a Palaeozoic succession consistent in age and composition with the coeval units of Central Iran (Rachidnejad-Omrani *et al.* 2002). In contrast, Ghasemi *et al.* (2002) identified in the southern part of the region, west of Hajiabad, a metamorphic complex consisting of garnet–gneiss amphibolite and anatectic granites that show Late Carboniferous 'Variscan' Ar–Ar ages ranging from 330 to 300 Ma. A possible Late Palaeozoic event followed by an Eo-Cimmerian deformation is also reported by Sengör (1990 and references therein) in the Khor-e Sefid Mountains east of the Neyriz ophiolites. Sheikholeslami *et al.* (2003), based on several new K–Ar radiometric ages and on structural analyses performed in this area, favour the occurrence of a unique Eo-Cimmerian metamorphic event, although older K–Ar ages of 310 $\pm$ 9 and 331 $\pm$ 5 Ma on single mineral phases belonging, respectively, to a metagabbro and to an anatectic granite were also found.

According to other interpretations (Sengör 1990; Bagheri & Stampli 2008), the SSZ was probably located more westward, and its present position

was achieved after the Triassic due to large left-lateral strike-slip orogen-parallel tectonic transport. However, detailed field structural data (Mohajjel & Fergusson 2000) describe important dextral transpression resulting from convergence during Tertiary and possibly also during Cretaceous times. In addition, Ghasemi & Talbot (2006) suggested at least 100 km of dextral shearing along recent faults between Arabia and the Zagros region.

Sengör (1990) hypothesized that the SSZ was part of a Carboniferous magmatic arc (the Podataksasi Zone) formed along the northern margin of Gondwana due to a presumed southward subduction of the Palaeotethys Ocean. According to this author, this presumed southwards subduction might also explain the opening of the Neotethys Ocean in a back-arc position between the Arabia, now represented by the Zagros belt, and the Cimmerian blocks. This hypothesis has been rejected by most of the authors for lack of geological evidence.

The SSZ is currently divided at the latitude of Golpayegan into a northern and southern portion with different features. The northern SSZ was only affected by an intra-continental rift filled with thick Triassic–Jurassic deposits, whereas the southern SSZ was separated from central Iran along the Nain–Baft Ocean from the Triassic onwards. Both, however, were separated from the Arabian Plate by the opening of Neotethys since the Early Permian. That separation is recorded by Upper Permian–Triassic ophiolites of the Sikhoran Complex (Geological Survey of Iran 1993; Ghasemi *et al.* 2002; Sheikholeslami *et al.* 2003; Ghasemi & Talbot 2006), exposed east of Hajiabad (Fig. 1). They include mafic–ultramafic layered intrusive rocks with a tholeiitic affinity that also record an Eo-Cimmerian deformation unconformably covered by Jurassic sediments.

According to Berberian & King (1981), the SSZ has remained the active margin of the Iran Plate since the end of the Triassic, and associate it with a subduction shift following the closure of the Palaleotethys Ocean to the north. Inversion of the oceanic basin began in the southern SSZ during Late Jurassic–Early Cretaceous (Neo-Cimmerian event), whereas in the northern part of the SSZ compressional deformation started during Cretaceous times.

Stratigraphic setting of Nakhlak

The record of a Triassic active margin crops out at Nakhlak in Central Iran (Fig. 3), in contrast with the carbonate-platform dominated sedimentation (Elikā Formation, Shotori Formation, etc.) that characterizes most of the Iranian region during the Early–Middle Triassic (Alavi *et al.* 1997; Seyed-Emami 2003; Balini *et al.* 2009). The approximately 2400 m-thick succession (Olenekian–Ladinian) of Nakhlak includes three main stratigraphic units. The base of the Triassic succession is not exposed; it is separated by an important low-angle fault zone from coarse-grained hornblende–gabbro in close associations with small patches of strongly serpentinized and altered ultramafic rocks (Fig. 4).

The Triassic at Nakhlak commences with the Olenekian–Anisian Alam Formation (1150 m thick), which consists of fine volcanic arenites, nodular limestones and marls with turbidites at the base. It was deposited in a marine setting and records a succession with alternating deepening and shallowing trends. The sedimentation was mostly volcaniclastic, but with three calcareous-dominated intervals. The upper part of the formation displays a shallowing-upwards trend passing into transitional–lagoonal sedimentation (*Unionites* assemblages) with increasing intercalations of fluvial conglomerates.

The ?Late Anisian–Ladinian Bāqoroq Formation, 870 m thick, represents an alluvial fan deposited in a fluvial environment. The unit thins out northward and changes composition, passing from conglomerates to sandstones. It documents the erosion of upper-crustal metasedimentary rocks. Detailed petrographic analyses of the Bāqoroq sandstones and clasts will be discussed later in order to compare their composition with the metamorphic rocks exposed to the south in the Anarak Massif.

The Late Ladinian, more than 370 m thick forms the Ashin Formation. It consists of fine-grained turbidites, and documents a rapid evolution from the continental and fluvial environment of the Bāqoroq Formation to a deep-water turbiditic system. Its age might reach up to the base of the Carnian (Alavi *et al.* 1997). The sandstone composition suggests a renewed volcaniclastic input, alternating with debris from metasedimentary rocks.

An Upper Cretaceous–Palaeogene succession, including massive limestones at the base, and followed by marly limestones and red sandstones at the top, unconformably covers the deformed Triassic units.

Structural setting of Nakhlak

Structural analyses have been performed in the Mesozoic successions of Nakhlak in the whole area of exposure (Fig. 4). The overall tectonic setting of the Nakhlak structure is shown in a general geological cross section based on our original field observations (Fig. 4). Structural investigations agree with the geological maps of Iran (Geological Survey of Iran 2003), and allow definition of the well-bedded Upper Cretaceous limestones that unconformably cover the deformed

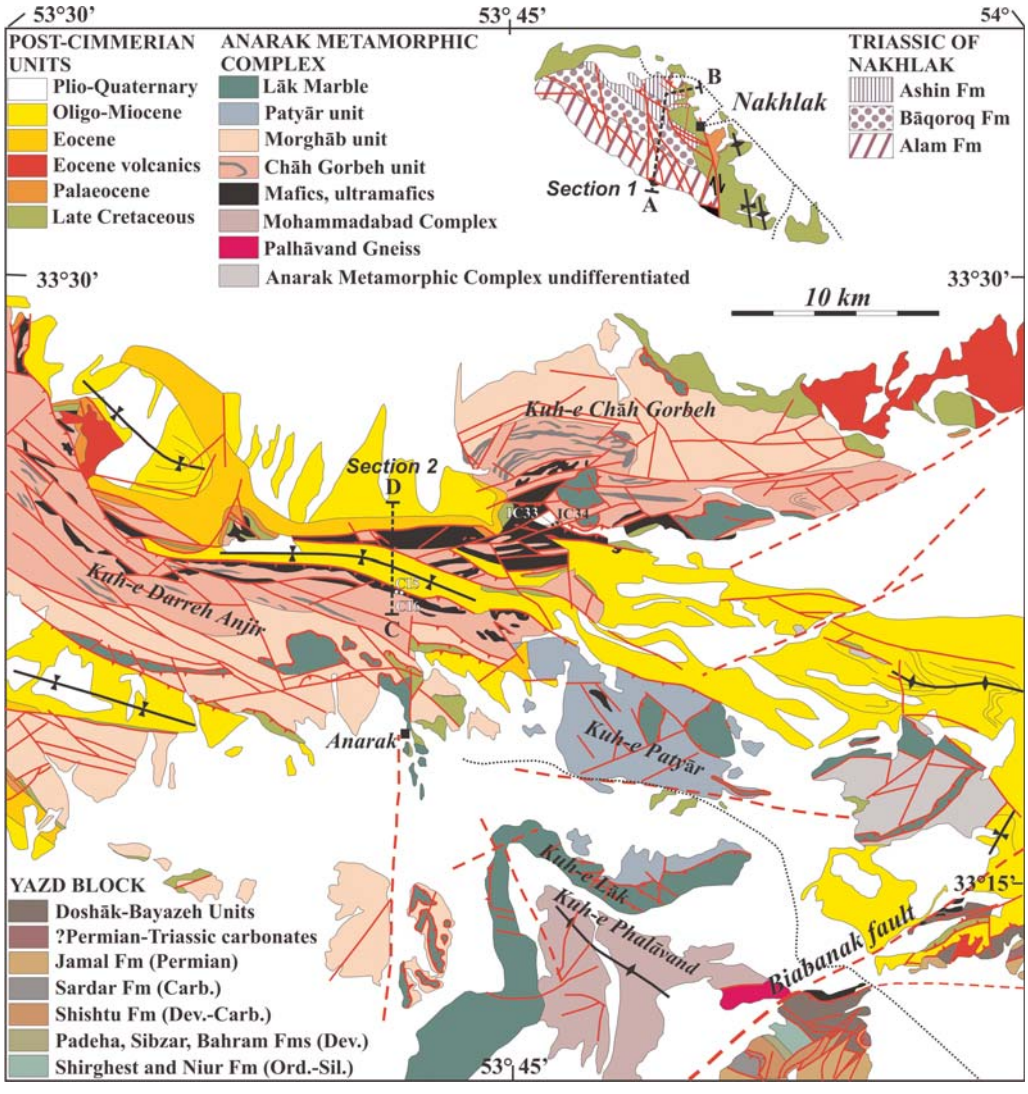

Fig. 3. Geological map of the Nakhlak–Anarak region, simplified from Geological Survey of Iran 1:250 000 and 1:100 000 maps of the region (Geological Survey of Iran 1984*a*, *b*, 2003), with the location of the two cross-sections of Figures 4 and 8. The locations of studied samples are also shown.

Triassic sequence (Figs 5A, B and 6A, D), contrary to what has been suggested by other authors (Alavi *et al.* 1997). Small reverse faults reactivating the discontinuity are observed only at local scale (Fig. 6B) and do not deform the contact between these units.

Our fieldwork shows that the Nakhlak structure is much more complex than previously described. The Triassic succession is affected by WNW–ESE-trending folds and reverse faults. In the southernmost part of the area, the Triassic succession is thrusted onto poorly exposed amphibole-metagabbros and serpentinites. These rocks are interpreted as a dismembered ophiolitic complex (Nakhlak-type ophiolites of Bagheri & Stampfli 2008), although no clear evidence for an oceanic lithosphere was given. The Upper Cretaceous beds also unconformably cover this mafic to ultramafic complex, indicating that they were juxtaposed to the Triassic successions before their deposition.

The southern part of the Nakhlak area shows the most complete succession that consists of the Alam, Bāqoroq and Ashin formations. A well-developed axial plane cleavage occurs in the southern part of

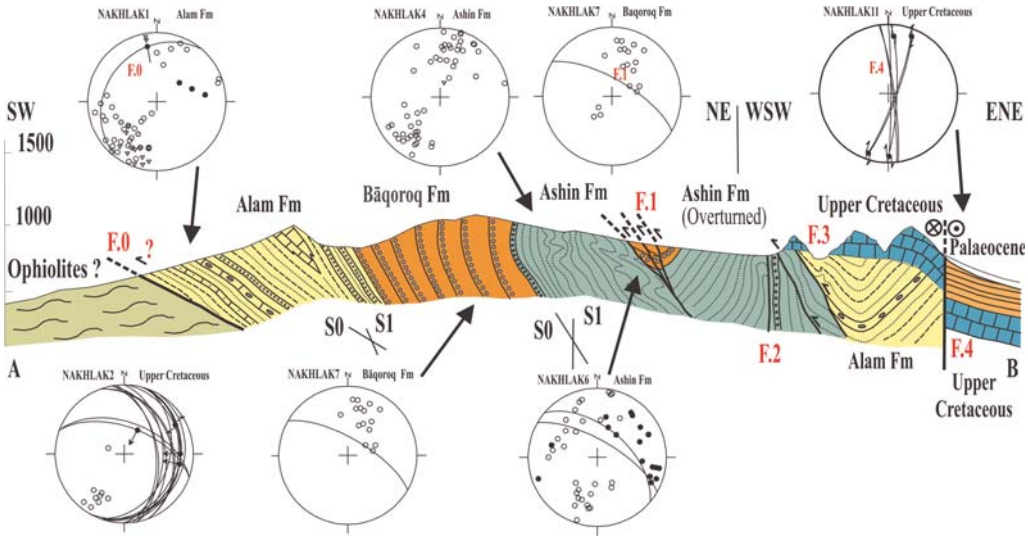

Fig. 4. Idealized geological cross section at Nakhlak, based on our original geological and structural observations; trace of the section in Figure 3. The topography is poorly constrained; vertical and horizontal scales are the same ones. Stereographic Schmidt's projections, lower hemisphere, refer to the measured structural elements. Faults are represented as cyclographic projections with black dots representing striations with relative sense of motion; small empty circles are poles to bedding; grey circles are poles to axial plane fracture cleavage; triangles are poles to axial planes; and fold axes are black small circles.

the area in the Alam Formation. A pressure-solution cleavage is present in the limestone beds, whereas a fracture cleavage formed in the marly layers of the upper part of the formation. Axial plane cleavage also strikes WNW–ESE and dips to NNE. In the central part of the Nakhlak area, the Ashin Formation shows complex disharmonic and conical folds with steeply plunging axes, possibly related to bedding-parallel detachments along shaly layers. Owing to these reasons, these folds cannot be used to determine the direction of tectonic transport.

The succession is interrupted northwards by an important WNW–ESE south-verging reverse fault. Tight folds in the footwall in the Ashin Formation show a strong dispersion of their axis trend (site Nakhlak 6; Fig. 4). This suggests that the folds formed before faulting and that they were reoriented due to the fault motion. In the hanging wall, the Bāqoroq and Ashin formations are completely overturned and show a small synformal structure parallel to the fault strike (Fig. 4). Overturned beds of the Ashin Formation are indicated by the orientation of flute casts; the overturned structure had been recognized several years ago by Holzer & Ghasemipour (1969). Present-day thickness of the Ashin Formation may reflect tectonic overthickening of the unit along both sides of the fault. To the north the Ashin Formation is crossed by strike-slip faults along which folds with vertical axes formed (Fig. 5B, 5C). In the northern part of the area, the Alam Formation overthrusts the Ashin Formation towards the south along another north-dipping high-angle reverse fault.

The Upper Cretaceous limestones unconformably cover most of the described structures. This suggests that folding and thrusting occurred between the Late Triassic and the end of the Early Cretaceous, and that these tectonic structures can be related to the Cimmerian orogeny *sensu latu*.

The Upper Cretaceous beds are weakly deformed. The limestones are affected by a N–S-trending asymmetric fold exposed along the east side of the area. The small N–S trending low-angle thrust faults that cut the unconformity in the southernmost part of the area can be interpreted as secondary shear structures related to the growth of the main fold.

An important N–S-trending strike-slip fault crosses all of the described structures. Mesoscopic structures record a dextral strike-slip motion of the fault (Fig. 6E). The strong hydrothermal circulation that occurs along the fault is possibly related to the formation of the galena–cerussite ore deposits (Holzer & Ghazemipour 1969) of the Nakhlak mine. The fault shows an important vertical offset of the Cretaceous beds (several hundred metres), which are in contact with Palaeocene red conglomeratic layers. This fault belongs to the system of large N–S- to NNE–SSW-trending right-lateral faults that cross central Iran (Walker & Jackson

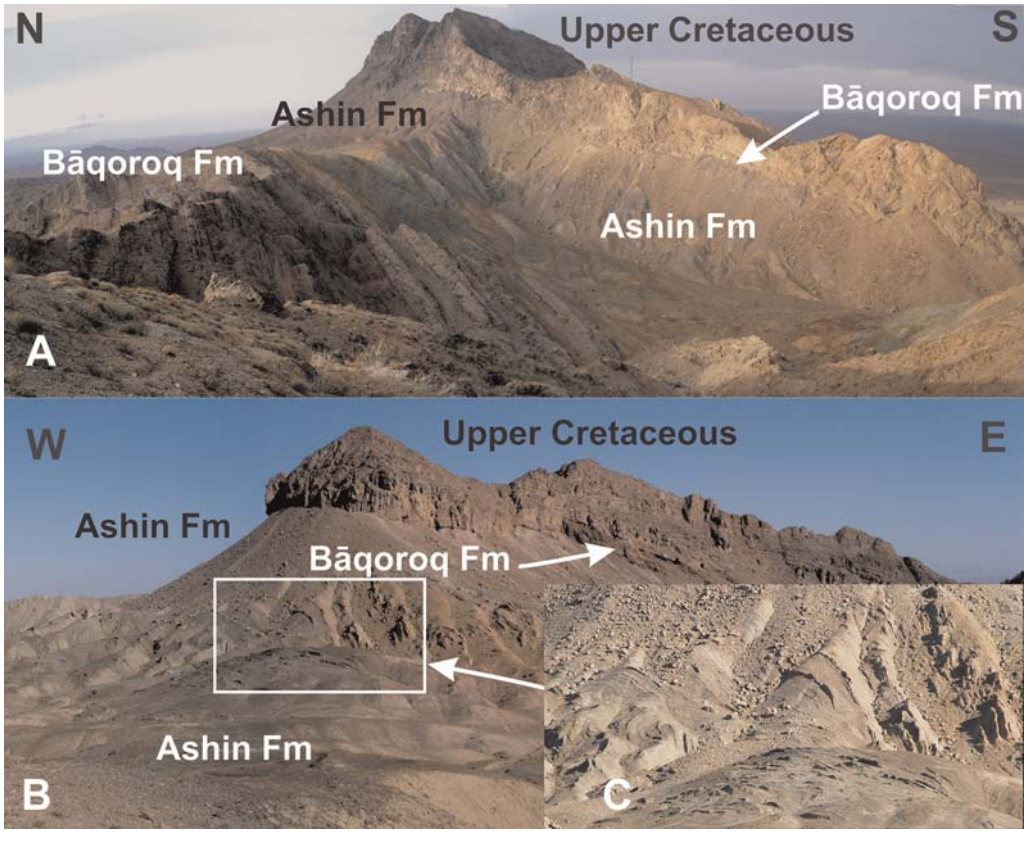

Fig. 5. Field views of the Nakhlak structure. Angular unconformity between the deformed Triassic succession and the Upper Cretaceous limestones in the southern (**A**) and northern part (**B**) of the area. Tectonic repetitions of the Bāqoroq Formation are evident below the unconformity in both views. (**C**) close view of the complex fold with vertical axes probably related to Tertiary strike-slip faults superposed to the Mesozoic tectonic structure.

2004). The fault extends between the active Deh Shir and Anar faults, which show a similar trend and kinematics (Walker & Jackson 2004). This N–S-trending right-lateral fault might be also related to the formation of the previously described N–S flexure, which can be interpreted as an in-line forced fold growing in a rigid basement before the final activation of the dextral shear zone. Examples of this kind are known along large strike-slip structures (Woodcock & Schubert 1995).

Petrography of Triassic Nakhlak sandstones

A detailed study of the petrography of the Nakhlak succession is reported in Balini *et al.* (2009) and is here summarized in its main results. Sandstones of the lower part of the Alam Formation are volcanic arenites dominated by microlithic–felsitic lithic fragments and plagioclase, and containing quartz, granophyric–granitoid rock fragments and chessboard albite. Such composition documents provenance from a magmatic arc dissected to various degrees, with sporadic contribution from encasing metamorphic wallrocks ('Magmatic Arc Provenance' of Dickinson 1985; Marsaglia & Ingersoll 1992; Garzanti *et al.* 2007). Relatively deep erosion levels within the arc massif are indicated by coarse-grained basal layers ('Dissected Arc' subprovenance), followed by overwhelming volcanic detritus indicating a major phase of intermediate volcanism ('Undissected Arc' subprovenance). Overlying sandstones include mica and metasedimentary rock fragments, pointing to an incision phase with subordinate supply from metamorphic wallrocks. A second volcanic cycle is suggested by overlying sandstones, initially derived largely from plagioclase-rich tuffs and next mainly including detritus from relatively mafic products. The unit is capped by sandstones relatively rich in quartz, chessboard albite, K-feldspar and

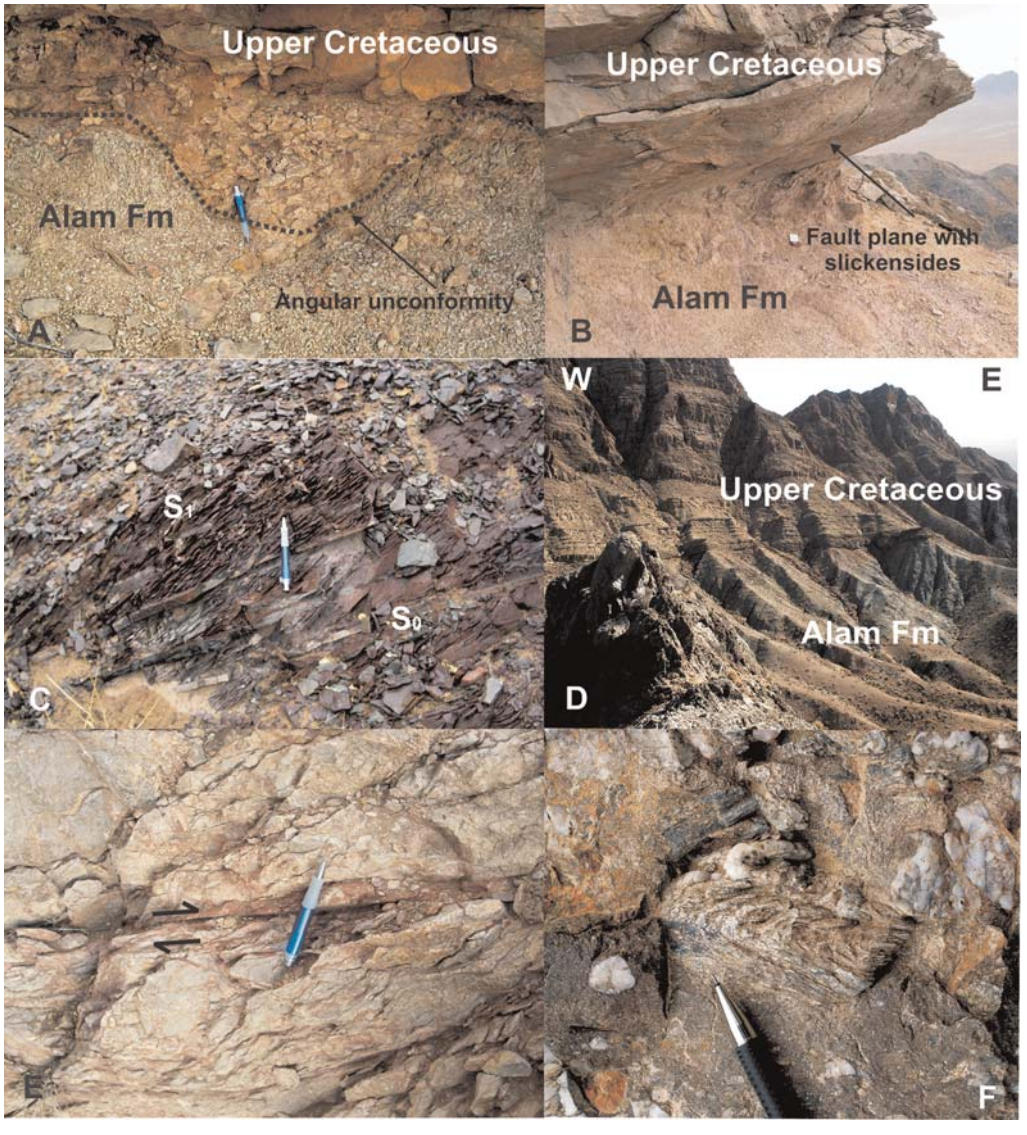

Fig. 6. Field views at Nakhlak. (**A**) Stratigraphic angular unconformity with a pronounced erosion channel between the Alam Formation and the Upper Cretaceous; (**B**) local tectonic reactivation of the same surface unconformity of (A); (**C**) fracture cleavage (S_1) in marly layers of the Alam Formation (S_0); (**D**) panoramic view of the unconformity between the Triassic Alam Formation and the Upper Cretaceous limestones in the southern part of the Nakhlak area; (**E**) dextral shearing along the strike-slip fault F.4 of Figure 4 indicated by oblique pressure-solution cleavage; and (**F**) clasts of metamorphic rocks in the upper bed of the Bāqoroq Formation (gneiss, greenschists, quartzites).

granophyric–granitoid rock fragments, suggesting a phase of ceased volcanism and renewed erosion.

Similar composition characterizes the basal layer of the overlying Bāqoroq Formation, whereas sandstones throughout the main body of the unit consist of quartz, metamorphic rock fragments, feldspars, granitoid rock fragments and micas, with only a few volcanic–subvolcanic rock fragments. Dominant medium-rank–high-rank schistose–gneissic rock fragments (metamorphic index (MI) 338 ± 15: Garzanti & Vezzoli 2003) indicate provenance from low-grade meta-sedimentary rocks (Fig. 6F). Such remarkably homogeneous quartzo-lithic metamorphiclastic composition documents a drastic change in provenance, revealing rapid erosion of a metamorphic

complex ('Recycled Orogen Provenance' of Dickinson 1985; 'Axial Belt Provenance' of Garzanti *et al.* 2007). Occurrence of serpentinite clasts suggested by Alavi *et al.* (1997) is not confirmed by our study.

The Ashin Formation includes mainly quartzolithic metamorphic clastic sandstones similar to those of the Bāqoroq Formation, intercalated with volcanic arenites. Volcanic arenites consist of virtually pure volcanic detritus, containing monocrystalline quartz with straight extinction and embayed or pyramidal outlines, and microlitic–vitric and pyroclastic grains, testifying to a phase of renewed intermediate–felsic explosive volcanism. Absence of sediments with mixed volcanic–metamorphic signatures (volcanic arenites invariably contain negligible amounts of metamorphic grains, and quartzo-lithic sandstones invariably include negligible amounts of volcanic detritus) indicate two different sources situated in geographically distinct areas.

Conglomerates are common in the upper part of the Alam Formation (Late Bythinian–Late Anisian), the Bāqoroq (Lower Ladinian) and the lower part of the Ashin Formation (Late Ladinian). Pebbles of quartz, metamorphic rocks and granitoids occur at the base of the Bāqoroq Formation, and become gradually more abundant upwards. Volcanic rocks are also common. Pebbles of sedimentary rocks are found only in the lower part of the Bāqoroq Formation. Field analysis of pebble composition is summarized in Figure 7.

Provenance interpretation

The petrography of Triassic Naklakh sandstones, interpreted in the framework of available stratigraphic and geological information, support the following considerations:

- the succession was deposited in a rapidly subsiding sedimentary basin during Early–Middle Triassic times;
- dominant magmatic arc provenance for Alam sandstones and some Ashin sandstones indicate deposition in an arc-related, supra-subduction setting;
- acidic–intermediate magmatism occurred in several distinct pulses, and was probably characterized by orogenic affinity varying irregularly in time from latite–andesite (lower Alam Formation) to basaltic andesite (upper Alam Formation) to dacite–rhyodacite (Ashin Formation);
- quartzo-lithic metamorphic clastic signatures for Bāqoroq sandstones and many Ashin sandstones may indicate provenance from a metamorphic axial zone of an orogenic prism, exhumed and eroded at Middle Triassic times (Late Anisian–Early Ladinian);
- active volcanic and metamorphic axial sources of detritus co-existed at Late Ladinian times, at opposite sides of the basin.

Based on such reconstruction, the Nakhlak succession is interpreted as deposited in a forearc

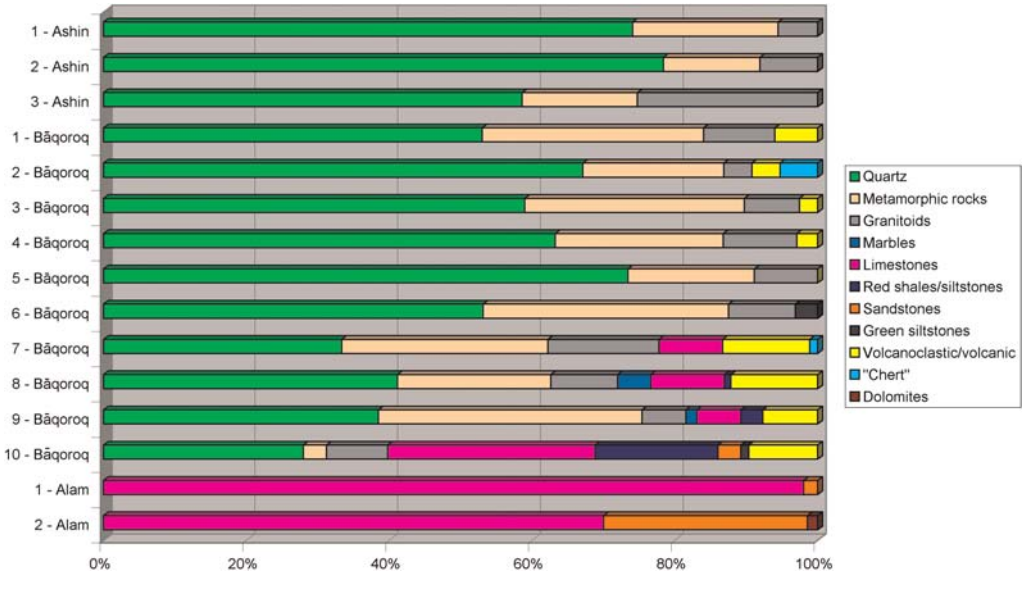

Fig. 7. Cumulative bar diagrams for the observed clast compositions in the Triassic of Nakhlak. Petrographic composition of the pebbles of the conglomerates of the upper part of the Alam, Bāqoroq and lower part of the Ashin formations.

basin. A significant orogenic event is suggested at Late Anisian times, when low-grade metamorphic rocks were exhumed and eroded. At Late Ladinian times, volcanism resumed in the magmatic arc.

The Anarak Metamorphic Complex and the metamorphic units of central Iran

The Anarak Metamorphic Complex (AMC), firstly described by Sharkovski *et al.* (1984), forms an east–west-trending mountain ridge that separates the Triassic of Nakhlak to the north from a continuous non-metamorphic Palaeo-Mesozoic sedimentary succession to the south. The succession to the south belongs to the Yazd block of Central Iran (Fig. 3). The sequence shows features similar to other Palaeozoic exposures described in North and Central Iran (Wendt *et al.* 2005; Leven & Gorgij 2006). The AMC trends E–W and is sharply juxtaposed westward against the 'Coloured Mélange' of the Nain–Baft Mesozoic ophiolites (Ghasemi & Talbot 2006) by the western termination of the Great Kavir Fault. To the east of Anarak, the AMC crops out discontinuously below the Meso-Cenozoic cover for about 150 km through Central Iran between Jandaq, Anarak and Khur (Fig. 2). It is associated with medium- to high-grade metamorphic rocks and ophiolitic remnants, exposed just south of the Great Kavir Fault (Bagheri & Stampfli 2008) (Fig. 2).

The AMC is subdivided into several subunits (Sharkovski *et al.* 1984), namely the Morghāb, Chāh Gorbeh, Kabudan, Patyār and Lāk Marble, which all show different metamorphic evolutions. The Chāh Gorbeh unit includes phyllites, mica schists and greenschists interlayered with thick marble layers and calcareous schists. Glaucophane- and lawsonite-schists are described in this unit (Sharkovski *et al.* 1984); blueschists also occur in the Patyār and Kabudan units, which have a similar composition and are exposed near Khur, 50 km to the east. The Lāk Marble includes a thick succession of meta-carbonates with a few metapelitic and quartzitic intercalations. Sharkovski *et al.* (1984) describe this unit as a large nappe exposed in isolated klippen overlying the other metamorphic units. A few remnants of archaeocyathids (*Paranacyathus sp.*, *Coscinocyathus sp.*, *Agastrocyathus sp.*, *Dicthyocyathus* sp.; Geological Survey of Iran 1984*a*) give an Early–?Middle Cambrian age to the Lāk Marble, whereas crinoids and gastropods dubitatively suggest a younger age (Sharkovski *et al.* 1984).

Mica schists, gneisses, orthogneisses and amphibolites form the Palhāvand Gneiss, which is separated by the Biabanak Fault from the Palaeozoic succession of the Yazd block exposed south of Anarak (Fig. 3).

Previously reported single phases and whole rock K–Ar radiometric ages (Sharkovski *et al.* 1984) are scattered between 420 and 208 Ma, with the main cluster between 300 and 375 Ma. The dates have been interpreted as the result of superposed Variscan and Late Triassic Cimmerian metamorphism. Triassic ages (222 ± 10 and 208 ± 8 Ma) have been reported by the same authors from the Kuh-e Dom Complex, which contains Palaeozoic fossils and is located NW of the Great Kavir Fault and of the Nain ophiolites (Fig. 2). Reyre & Mohafez (1970) obtained a Rb–Sr 203 ± 13 Ma radiometric age from metamorphic rocks of the AMC around Anarak, which also suggests a Late Triassic metamorphism. Evidence of possible Precambrian protholiths in the AMC is given by a Rb–Sr age determination of 845 Ma (Reyre & Mohafez 1970). Additional stratigraphic constraints on the age of deformation of the AMC occur in the Khur area. Here the Shemshak Group overlies the AMC and related units affected by low-grade metamorphism with sharp non-conformity, suggesting an important Eo-Cimmerian tectono-metamorphic event (Sharkovski *et al.* 1984). In the whole region, a successive Neo-Cimmerian event is marked by the deposition of the Low Cretaceous Chāh Palang Conglomerate lying with a strong angular unconformity on older units, including the Shemshak Group. A very low-grade metamorphic overprint on the Shemshak and Middle–Late Jurassic granitic rocks (Geological Survey of Iran 1972, 1976) around Torud, to the north and SW of Yazd (Fig. 2), suggests an even later thermal event.

Elongated slivers of mafic and ultramafic rocks ('Anarak-type ophiolites' of Bagheri & Stampfli 2008), up to 5 km wide and 20 km long, are tectonically intercalated within the metamorphic rocks of the AMC. Ultramafic rocks occur especially along the northern slopes of the Anarak Massif. Small patches of serpentinites also crop out just to the north of the Biabanak Fault in the southern part of the area (Fig. 3). Most of the rocks can be classified as serpentinized harzburgite and olivine orthopyroxenite, occasionally with layered structures (Sharkovski *et al.* 1984). Undeformed plagiogranite (trondhjemite), quartz-diorite and tonalite occur as well. Bagheri & Stampfli (2008) report a 262 ± 1 Ma U–Pb zircon age for a trondhjemite intruded in the Chāh Gorbeh unit, and consider that it predates the blueschists-facies metamorphism of the unit.

Bagheri & Stampfli (2008) proposed a significantly new scenario, which implies the occurrence of a polyphase accretionary wedge that underwent metamorphism during Carboniferous times ('Variscan event'), and also subsequent deformation during Permian and Triassic times in the region

south of the Great Kavir Fault. The Lāk Marble, the Patyār unit and the ophiolitic remnants ('Anarak-type ophiolites') in this reconstruction represent the relicts of a seamount characterized by an oceanic basement (ultramafic and metavolcanic rocks of the 'Anarak-type ophiolites') overlain by reefal carbonates (Lāk Marble). Metadolomites, metacherts and schists of the Patyār Unit represent the former lagoonal deposits and the successive pelagic sedimentary cover deposited after the drowning of the atoll. The same authors also question previous findings of Cambrian archaeocyathids (Sharkovski *et al.* 1984), although no alternative indication of the age of the reefal carbonates of the Anarak Seamount is given.

According to Bagheri & Stampfli (2008), the Morghāb schists and the blueschists of Chāh Gorbeh unit form an accretionary wedge located along the southern active margin of the Eurasian Plate (Turan domain). The Anarak Seamount (Lāk Marble and Patyār unit) and the nearby Kabudan Guyot were partly subducted, metamorphosed and accreted into the wedge during either Permian or Triassic time. New radiometric Ar–Ar ages (Bagheri & Stampfli 2008) obtained on white micas constrain the presence of an older 'Variscan' *sensu latu* metamorphism in the Morghāb Schists unit (333–320 Ma), also exposed east of Jandaq (Fig. 2), and of a younger event poorly dated between 280 and 232 Ma in the Chāh Gorbeh unit, respectively from Ar–Ar dating of crossite and stilpnomelane.

A new element introduced by Bagheri & Stampfli (2008) concerns the age and significance of the Doshākh and the Bayazeh units, previously interpreted as a greenschists-facies Precambrian or Lower Palaeozoic metamorphic basement of the Yazd block (Sharkovski *et al.* 1984). According to Bagheri & Stampfli (2008), the Doshākh unit has given a Middle Permian–Middle Triassic age based on conodonts, and it is now interpreted as a part of the accretionary wedge developed after the collision of the Anarak seamount (Bagheri & Stampfli 2008). The Bayazeh Flysch forms a distal turbidite unit related to the same Permo-Triassic wedge, recording the final closure of the subduction-related basin.

New geological observations in the Anarak area

The Anarak Massif was investigated along the main road that crosses the high mountain chain north of Anarak, reaching the locality of Chāh Gorbeh (Figs 3, 8 and 9A), in order to define the main structural features of the Anarak Metamorphic Complex (AMC) and its relationships with the Meso-Cenozoic units cropping out to the north. The Chāh Gorbeh unit consists here of an association of marbles, metapelites and metabasites which are

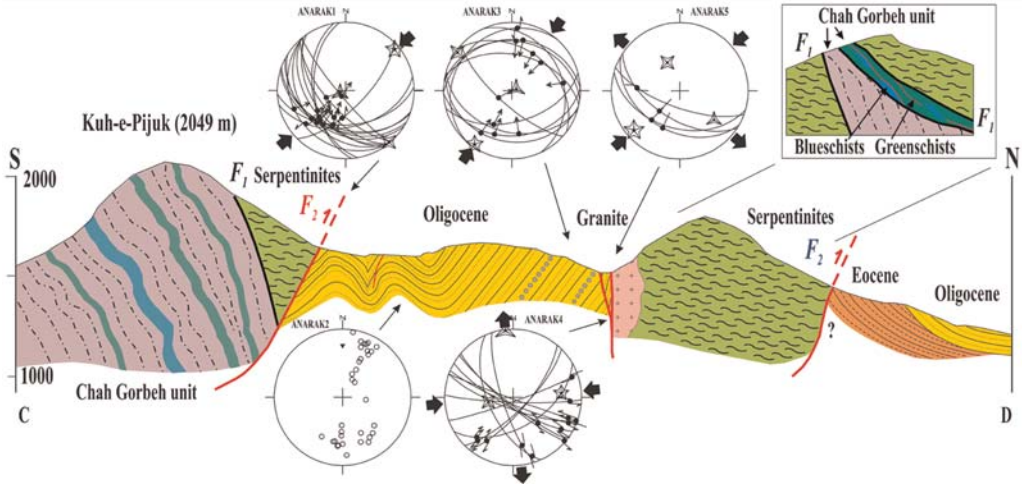

Fig. 8. Geological cross section at Anarak; trace of the section in Figure 3. The topography is poorly constrained; vertical and horizontal scales are the same ones. F_1, older faults possibly related to the growth of the Eo-Cimmerian accretionary wedge; F_2, late Tertiary faults. Stereoplots as in Figure 4. Convergent arrows correspond to the horizontal direction of the σ_1 axis; divergent arrows to the horizontal direction of the σ_3 axis. Stress axes are represented as stars with five (σ_1), four (σ_2) and three branches (σ_3) obtained with inversion of fault populations using the inversion methods proposed by Angelier (1984, 1990). The small sections in the rectangle is a lateral variation of the main one observed south of Kuh-e Chāh Gorbeh.

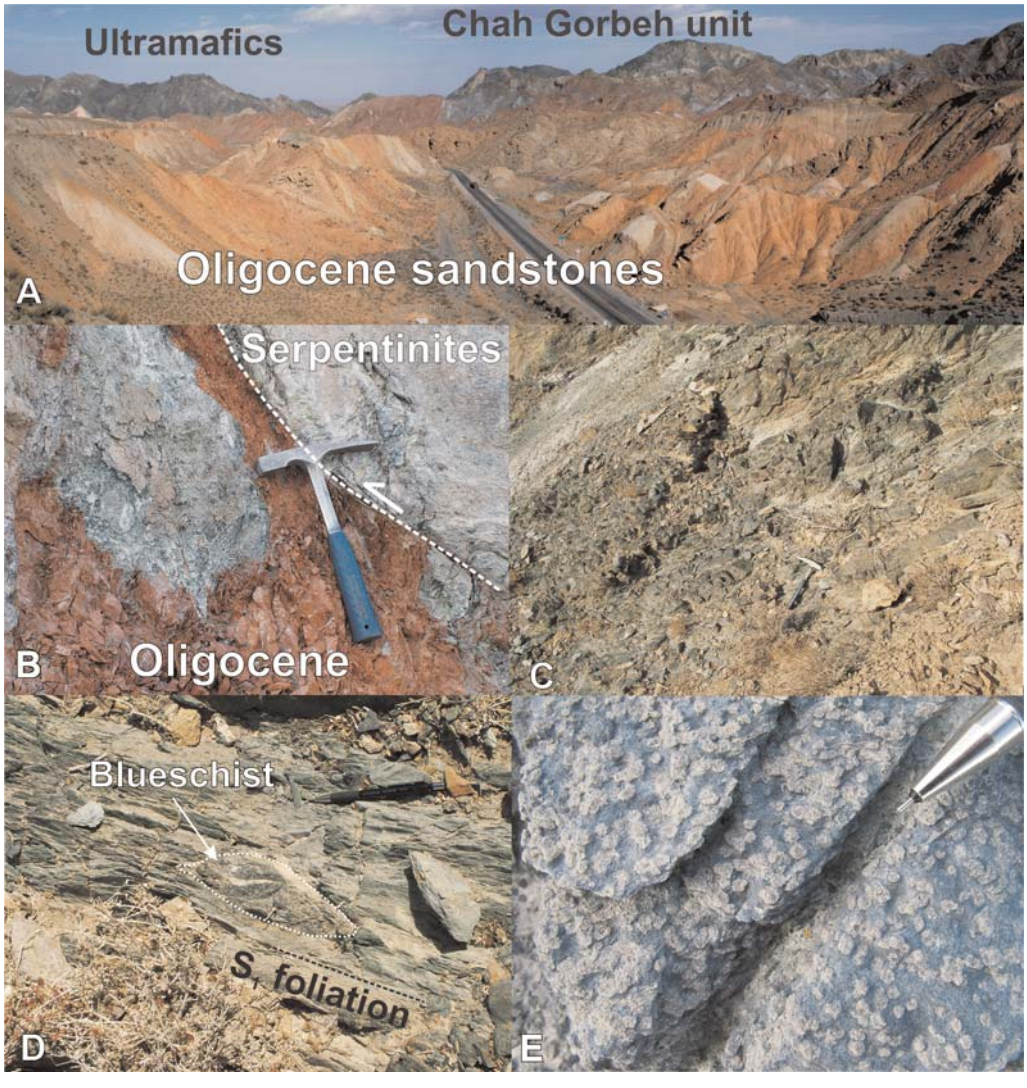

Fig. 9. Field views of the Anarak Metamorphic Complex. (**A**) Northward view across the Anarak Massif along the main road; compare with the section of Figure 8; (**B**) thrust contact between the serpentinitic slivers occurring in the AMC and the Oligocene sedimentary deposits; (**C**) blueschists of the Chāh Gorbeh unit, possibly showing relicts of pillow lava structures; (**D**) blueschist boudins in a greenschist matrix, Chāh Gorbeh unit; and (**E**) pseudomorph aggregates on plagioclase phenocrystals, Chāh Gorbeh unit.

juxtaposed to strongly serpentinized ultramafic rocks by a steep north-dipping fault (Figs 8 and 9B). Both units overthrust a folded terrigenous succession mainly consisting of Eocene to (poorly constrained) Lower Miocene beds, including red marls and sandstones with discontinuous conglomeratic layers. Faults developed along the contact suggest a NE–SW direction of horizontal compression, consistent with the trends of fold axes developed within the Tertiary sediments. The northern boundary of the Tertiary outcrops is also faulted, showing reverse faults with the same trends and conjugate strike-slip faults overprinting the contact with a well-preserved granitoid intrusive. A different structure was observed along another cross-section located to the east of the main road, where the Chāh Gorbeh unit is exposed. Along this section, a thin slice of blueschists is sandwiched between two serpentinitic layers that show north-dipping tectonic boundaries. Blueschists occur in

metabasites, possibly representing a succession of meta-lava flows (Fig. 9C, D).

Petrography of the Anarak Metamorphic Complex

We focused on two key rock associations that can give important insights into the evolution of the AMC: blueschists of the Chāh Gorbeh unit and ultramafic rocks.

Blueschists and greenschists of the Chāh Gorbeh unit. Blueschists occur in the Chāh Gorbeh unit, forming small decimetric boudins possibly representing deformed pillow lavas; boudins are embedded in a foliated matrix consisting of epidote–amphibole–chlorite schists (Fig. 9C, D).

Blueschists are very fine grained (crystal size <2 mm) and display a S-tectonic texture with a pervasive foliation marked by the preferred shape orientation of amphibole and chlorite. They contain amphibole, chlorite, plagioclase, white mica, quartz, titanite, rutile, apatite with subordinate calcite, hematite and sulphides. A pervasive foliation (S_1) is defined by blue-lavender amphibole and chlorite; white mica is aligned parallel to the S_1 only in a few samples, whereas it commonly forms spherulitic aggregates bordered by a thin titanite corona (Fig. 10A). White mica is oriented in both random and radial directions within the spherulitic aggregates (Fig. 10B). Deflection of the S_1 foliation around the aggregates indicates that they predate the foliation.

A pervasive post-S_1 crystallization of randomly oriented blue–green amphibole and chlorite occurs in several samples, probably indicating a transition from blueschist- to greenschist-facies conditions.

The equilibrium phase assemblage for the blueschist pressure–temperature (P–T) conditions includes amI + chlI + wmcaII + qtz + ttn + plI + hem (all mineral abbreviations after IUGS recommendations). AmI has a composition varying from Mg-riebeckite to glaucophane, depending on the Al/Fe^{3+} ratio (Table 1). A general trend from Mg-riebeckitic toward glaucophanic composition from core to rim (i.e. increase in the Al/Fe^{3+} ratio) was observed within larger amphibole crystals (Fig. 11A, B). The K content is close to zero, whereas low amounts of Ti and Mn have been detected (0.02 atoms per formula unit (apfu)) displaying no correlation with Al/Fe^{3+} and X_{Mg} (Table 2).

AmII, growing statically with no preferred orientation together with chlII, has an actinolitic composition. White mica, wmcaII, aligned parallel to the S_1 foliation has a phengitic composition with Si comprised between 3.5 and 3.6 apfu and X_{Mg} close to 0.68 apfu (Fig. 11C and Table 2). Significant amounts of Ti (0.04 apfu) and Cr (0.02 apfu) have been detected in several crystals. White mica, wmcaI, forming the pre-S_1 spherulitic aggregates, have Si contents around 3.4 apfu, slightly lower than wmcaII.

Plagioclase in textural equilibrium with the syn-S_1 phase assemblage displays an albitic composition (Ab_{98}) close to the end-member. Thin rims of Ca-rich plagioclase ($Ab_{95}An_{05}$), plII, where observed to grow on plgI where the static crystallization of post-S_1 amII and chlII is more intense.

Chlorite shows no significant compositional variations as both chlI, grown synkinematically to S_1, and chlII, grown statically with amII, have similar compositions to X_{Mg} close to 0.70 apfu.

As previously described, titanite forms thin coronae, no more than 0.2–0.3 mm in width,

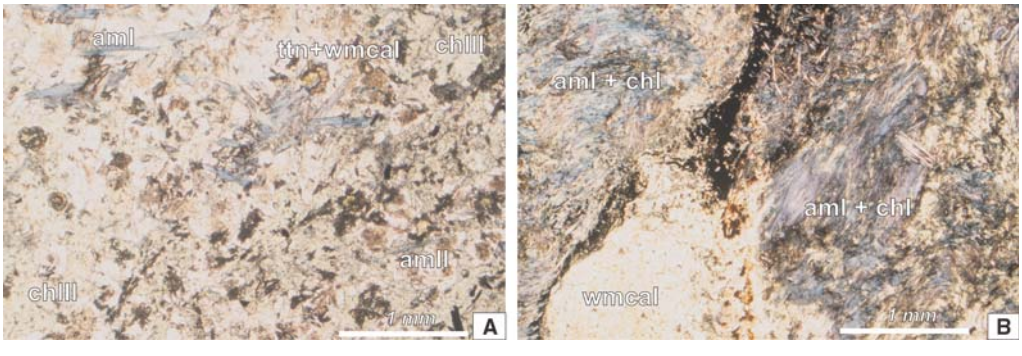

Fig. 10. Photomicrographs of blueschists from the Chāh Gorbeh unit of the Anarak Metamorphic Complex. Am, blue-amphibole; ch, chlorite; ttn, titanite; wmca, white mica. I, II, II refer to the different phase assemblages; see text for discussion. (**A**) Spherulithic aggregates of WmcaI rimmed by titanite coronae within a fine-grained matrix made by acicular bluish amphibole, chlorite and plagioclase; (**B**) WmcaI aggregates embedded within a fine-grained matrix in which the S_1 foliation is visible in the right part of the image.

Table 1. *Mineral chemistry of the amphiboles in the blueschists of the Anarak Metamorphic Complex, Chāh Gorbeh Unit. Location of samples IC33 and IC34 given in Figure 3*

Sample	IC33	IC33	IC33	IC33	IC34	IC34	IC34	IC34	IC33	IC33	IC33	IC34
Phase	ampI	ampI	ampI	ampI	ampI	ampI	ampI	ampI	ampII	ampII	ampII	ampII
SiO_2	55.86	57.45	57.27	57.53	56.41	56.75	56.36	56.15	51.34	53.49	52.72	50.95
TiO_2	0.07	0.04	0.06	0.01	0.11	0.15	0.11	0.14	0.05	0.04	0.02	0.01
Al_2O_3	2.7	3.24	3.21	3.77	2.63	3.07	2.46	2.66	2.02	2.06	2.15	1.96
Cr_2O_3	0	0.05	0.03	0.06	0.08	0.01	0.04	0.04	0.01	0.04	0.01	0.01
Fe_2O_3	11.73	11.23	11	10.22	12.62	11.88	13.49	14.28	11.41	7.19	8.21	10.77
FeO	7.16	7.67	7.75	8.26	7.96	8.24	7.54	7.1	2.45	5.77	5.7	2.99
MnO	0.13	0.15	0.11	0.12	0.1	0.12	0.07	0.11	0	0.01	0.01	0.02
NiO	0.01	0.04	0.01	0.04	0.05	0.01	0	0.05	0	0.01	0.01	0.01
MgO	11.4	10.93	11.21	10.74	10.34	10.02	10.42	10.28	16.12	15.73	15.75	16.03
CaO	2.55	1.06	1.02	0.77	0.88	1.21	1.01	0.88	10.46	10.46	10.56	10.78
Na_2O	5.96	6.8	6.67	6.85	6.8	6.86	6.82	6.93	1.87	1.83	1.61	1.6
K_2O	0.04	0.02	0.03	0.01	0.04	0.03	0.02	0.01	0.03	0.02	0.03	0.03
Total	97.61	98.68	98.37	98.38	98.02	98.35	98.34	98.63	95.76	96.65	96.78	95.16
Si	7.957	8.056	8.050	8.075	8.022	8.034	7.996	7.951	7.46	7.68	7.59	7.46
Ti	0.007	0.004	0.006	0.001	0.012	0.016	0.011	0.015	0.01	0.00	0.00	0.00
Al	0.453	0.535	0.532	0.624	0.441	0.512	0.411	0.444	0.35	0.35	0.37	0.34
Cr	0.000	0.005	0.003	0.006	0.009	0.001	0.005	0.004	0.00	0.00	0.00	0.00
Fe^{3+}	1.257	1.185	1.164	1.079	1.351	1.266	1.441	1.521	1.25	0.78	0.89	1.19
Fe^{2+}	0.853	0.899	0.911	0.969	0.947	0.976	0.895	0.841	0.30	0.69	0.69	0.37
Mn	0.016	0.017	0.013	0.015	0.012	0.015	0.008	0.013	0.00	0.00	0.00	0.00
Ni	0.001	0.005	0.001	0.004	0.006	0.001	0.000	0.005	0.00	0.00	0.00	0.00
Mg	2.420	2.284	2.349	2.247	2.192	2.114	2.204	2.170	3.49	3.37	3.38	3.50
Ca	0.389	0.160	0.153	0.116	0.135	0.183	0.154	0.133	1.63	1.61	1.63	1.69
Na	1.646	1.849	1.818	1.864	1.875	1.883	1.876	1.903	0.53	0.51	0.45	0.45
K	0.007	0.003	0.006	0.003	0.007	0.005	0.005	0.002	0.01	0.00	0.01	0.01
Cation	15.007	15.003	15.006	15.003	15.007	15.005	15.005	15.002	15.006	15.004	15.006	15.006
X_{Mg}	0.534	0.523	0.531	0.523	0.488	0.485	0.486	0.479	0.693	0.696	0.682	0.693
Na_B	1.611	1.840	1.818	1.864	1.865	1.817	1.846	1.867	0.372	0.39	0.371	0.309

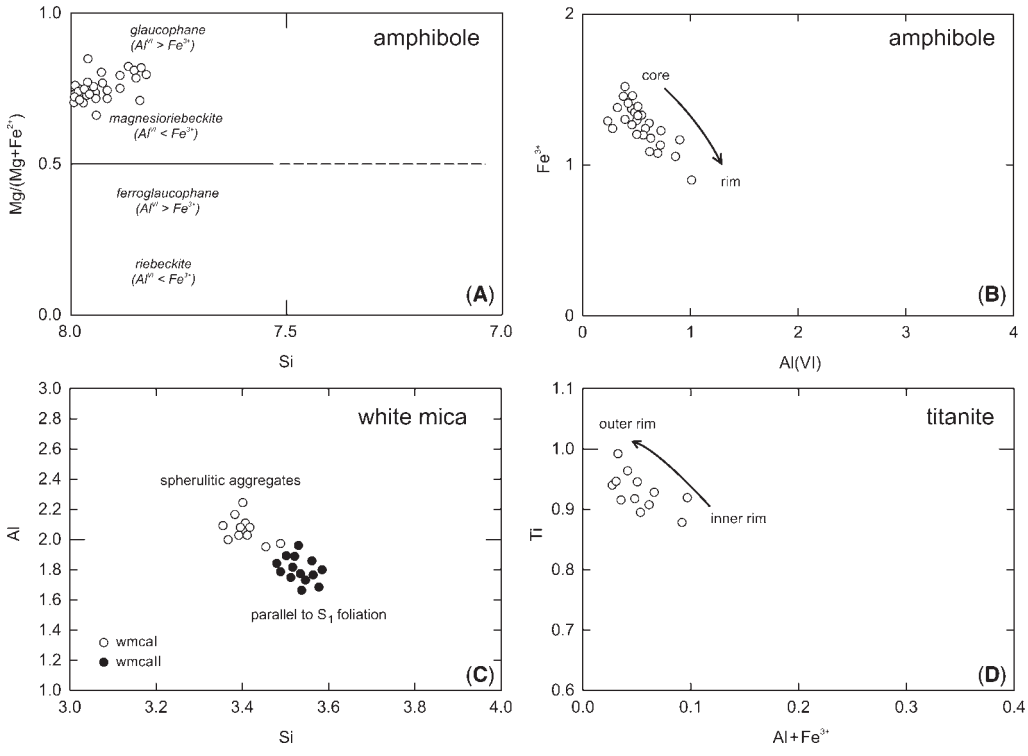

Fig. 11. Compositional variations of (**A**) and (**B**) amphibole, (**C**) white micas and (**D**) titanites from the blueschists of the Chāh Gorbeh unit. AmI are substantially Mg-riebeckits and display a variation trend towards glaucophanic compositions from core to rim. Micas parallel to the S_1 foliation (wmcaII) have a higher Si content with respect to wmcaI. Titanites show a weak compositional zoning with Ti/(Al + Fe^{3+}) ratio increasing towards the outer rim.

around wmcaI aggregates. A loosely defined compositional zoning of ttn coronae going from the inner rim, in contact with wmcaI, to the outer rim, in contact with the syn-S_1 phases, was observed (Fig. 11D); zoning is individuated by an increase of Ti (from 0.9 to 1 apfu) and decrease of Al + Fe^{3+} from 0.12 to 0.02 apfu.

Estimate of the peak metamorphic conditions for the blueschists of the Chāh Gorbeh unit is not straightforward, as the syn-S_1 phase assemblage, in the absence of both epidote and lawsonite, is loosely constrained in the P–T field. An upper pressure limit is posed by the absence of omphacitic clinopyroxene, which constrains the peak pressure for the syn-S_1 assemblage below 1.2 GPa. In addition, a lack of aragonite in the S_1 paragenesis, indicating that calcite was the stable carbonate phase during peak conditions, constrains the upper pressure boundary to 0.8–0.9 GPa. An upper temperature limit is also provided by the absence of garnet (Apted & Liou 1983; Guiraud *et al.* 1990), which is stable above 400–450 °C for pressure conditions ranging between 0.4 and 0.9 GPa.

The absence of lawsonite could be tentatively used as a lower temperature boundary, confining the peak phase mineral assemblage with Na-amphibole, albite, white mica, chlorite and titanite at a temperature above 300 °C for a 0.4–0.9 GPa pressure range.

The pressure peak recorded by the syn-S_1 phase assemblage was followed by a decrease in pressure and an increase in temperature, suggested by the crystallization of actinolitic amphibole and chlorite and the growing of thin rims of Ca-rich plgII on plI. This suggests that the blueschists of the Chāh Gorbeh unit were subducted into an accretionary wedge at a depth of at least 15–20 km.

Serpentinized peridotites. Ultramafic rocks have been sampled along the main road from Anarak to the north. Here they are almost completely serpentinized, preserving only sparse relicts of primary phase assemblages (Fig. 12A). Serpentinites display a schistose texture, with isolated domains showing a preserved massive texture. Clinopyroxene, olivine and spinel relicts have been found in these domains,

Table 2. *Mineral chemistry of white micas, chlorite, titanite and plagioclase within the blueschists of the Anarak Metamorphic Complex, Chāh Gorbeh Unit. Location of samples IC33 and IC34 is given Figure 3*

Sample	IC33	IC33	IC33	IC33	IC34	IC33	IC33	IC33	IC34	IC34	IC33	IC33	IC34	IC34
Mineral	wmII	wmII	wmI	wmII	wmII	chlI	chlI	ttn	ttn	ttn	plgI	plgI	plgI	plgI
SiO_2	51.35	51.59	48.4	52.01	52.62	29.79	30.15	31.68	31.85	31.54	69.46	68.94	69.56	69.47
TiO_2	0.29	0.27	0.8	0.39	0.32	0.03	0.04	37.02	37.37	38.17	0.00	0.03	0.02	0.02
Al_2O_3	22.44	21.64	18.63	20.62	21.99	18.13	17.99	1.43	1.2	0.5	19.48	19.29	19.38	19.51
Cr_2O_3	0.15	0.23	0.28	0.21	0.15	0.11	0.14	0	0.01	0.05	0.00	0.00	0.01	0.04
Fe_2O_3	0	0	0	0	0	0	0	0.24	0.16	0.33	0.00	0.00	0	0
FeO	3.98	4.91	8.33	5.13	4.05	16.72	17.1	0.44	0.62	0.35	0.16	0.41	0.5	0.4
MnO	0.04	0.06	0.07	0.04	0.05	0.32	0.29	0.03	0.01	0.05	0.02	0.00	0	0.01
NiO	0	0	0	0	0	0.03	0.07	0	0	0	0.03	0.00	0	0
MgO	4.86	5.84	8.53	6.17	4.85	22.39	22.57	0.05	0.05	0.03	0.02	0.04	0.08	0.03
CaO	0	0	0	0	0	0.12	0.13	27.88	27.79	27.98	0.00	0.04	0.06	0.05
Na_2O	0.06	0.04	0.06	0.05	0.05	0.06	0.07	0.15	0.16	0.07	11.56	11.66	11.78	11.73
K_2O	10.99	10.27	10.02	10.53	10.81	0.1	0.09	0.05	0.05	0.05	0.04	0.04	0.03	0.02
Total	94.16	94.85	95.12	95.15	94.89	87.8	88.64	98.97	99.27	99.12	100.78	100.45	101.42	101.28
Si	3.516	3.512	3.381	3.540	3.565	6.001	6.022	1.032	1.036	1.032	3.018	3.003	3.001	3.002
Ti	0.015	0.014	0.042	0.020	0.016	0.005	0.006	0.907	0.914	0.939	0.000	0.001	0.001	0.001
Al	1.811	1.736	1.534	1.654	1.756	4.304	4.235	0.055	0.046	0.019	0.998	0.990	0.985	0.994
Cr	0.008	0.012	0.016	0.011	0.008	0.018	0.022	0.000	0.000	0.001	0.000	0.000	0.000	0.001
Fe^{3+}	0.000	0.000	0.000	0.000	0.000	0.000	0.000	0.006	0.004	0.008	0.000	0.000	0.000	0.000
Fe^{2+}	0.228	0.280	0.487	0.292	0.229	2.817	2.857	0.012	0.017	0.010	0.006	0.015	0.018	0.015
Mn	0.002	0.004	0.004	0.002	0.003	0.055	0.049	0.001	0.000	0.001	0.001	0.000	0.000	0.000
Ni	0.000	0.000	0.000	0.000	0.000	0.005	0.011	0.000	0.000	0.000	0.001	0.000	0.000	0.000
Mg	0.496	0.593	0.888	0.626	0.490	6.722	6.720	0.002	0.002	0.002	0.001	0.003	0.005	0.002
Ca	0.000	0.000	0.000	0.000	0.000	0.026	0.028	0.973	0.968	0.981	0.000	0.002	0.003	0.002
Na	0.008	0.005	0.008	0.007	0.007	0.023	0.027	0.010	0.010	0.004	0.974	0.985	0.985	0.983
K	0.960	0.892	0.893	0.914	0.934	0.026	0.023	0.002	0.002	0.002	0.002	0.002	0.002	0.001

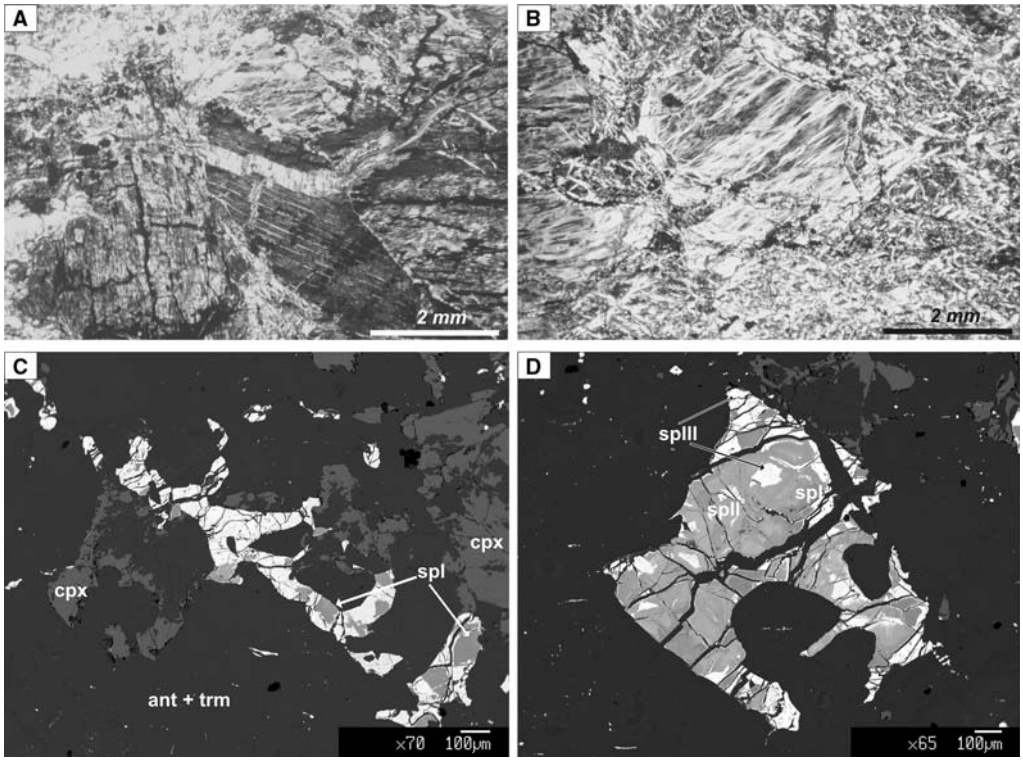

Fig. 12. (**A**) Photomicrograph of serpentinized peridotite from the Chāh Gorbeh unit showing bastite pseudomorphs after pyroxenes; (**B**) bastites within a matrix displaying mesh to interpenetrating textures; (**C**) back scattered electrons/scanning electron microscope (BSE/SEM) image of an ameboid spinel porphyroclast and clinopyroxene relicts within a tremolite + antigorite matrix; and (**D**) BSE/SEM image of complex chemical zoning within a spinel porphyroclast. ant, antigorite; cpx, clinopyroxene; sp, spinel; trm, tremolite.

whilst only chromian spinel porphyroclasts are present in the schistose ones.

Schistosity is defined by the preferred orientation of antigorite, replacing bastites of lizardite and chrysotile on primary olivine and pyroxene. Mesh and interpenetrating textures are common in several samples (Fig. 12B).

Preserved spinel grains display an amoeboid habit with complex compositional zoning (Fig. 12C, D). In many cores an Al-rich spinel is preserved (sp I, dark grey) with Cr# (Cr# = molar[100*Cr/(Cr + Al)]) 0.14–0.16, $Fe^{3+}/(Al + Cr + Fe^{3+}) < 0.1$ and Ti content close to zero, representing, possibly, a primary phase (Dick & Bullen 1984). Successive re-equilibrations are indicated by overgrowth rims progressively richer in Fe and depleted in Cr (Table 3). The surrounding dark-grey matrix mainly consists of antigorite and tremolite with minor amounts of chlorite.

Rare olivine relicts preserved at the core of pseudomorphs with mesh texture have a Fo_{94} composition with small amounts of Cr (0.04 Cr_2O_3 wt%), Mn (0.20 MnO wt%) and Ni (0.11 NiO wt%).

Clinopyroxene relicts, observed in one sample, display irregular shapes, varying with the degree of substitution by tremolite and antigorite. Their chemical composition is close to the diopside end-member, with amount of Na and Al close to zero (Table 4). Tiny intergrowths of tremolite and a sodic–calcic amphiboles are observed around some clinopyroxene relicts. The presence of such reaction rims may indicate an increase in pressure, consistent with the metamorphic evolution suggested for the blueschists of the Chāh Gorbeh unit.

Discussion

Petrographic and geological data on the Nakhlak–Anarak region provide several constraints for the reconstruction of the Triassic geodynamic evolution of Central Iran. They suggest that the Nakhlak succession was deposited in a forearc setting to the north of a subduction zone. Intermittent stages of volcanic activity alternating with uplift and erosion may indicate oblique convergence and

Table 3. *Mineral chemistry of spinels contained in the ultramafics of the Anarak Metamorphic Complex. Location of samples CI5 and CI6 is given in Figure 3*

Sample	CI5	CI5	CI6	CI6	CI6	CI5	CI6
Phase	sp1	sp1	sp1	sp2	sp2	sp3	sp3
SiO_2	0.03	0.04	0.05	0.21	1.63	0.66	0.83
TiO_2	0.04	0.03	0.04	0.09	0.53	0.14	0.13
Al_2O_3	52.87	51.88	52.76	0.13	0.2	0.09	0.13
Cr_2O_3	15	15.32	14.89	7.13	9.25	3.79	4.5
Fe_2O_3	0.06	0.2	0.67	60.63	55.36	64.2	62.99
FeO	11.16	11.47	10.73	29.36	28.07	29.55	29.37
MnO	0.1	0.13	0.12	1.06	1.77	0.58	0.67
NiO	0.27	0.29	0.32	0.12	0.28	0.1	0.16
ZnO	0	0	0	0	0	0	0
MgO	18.48	17.98	18.79	0.45	1.99	0.99	1.05
CaO	0	0	0	0.04	0.06	0.04	0.19
Na_2O	0.01	0.02	0.01	0	0.09	0.09	0.08
K_2O	0	0	0	0	0	0	0
Total	98.03	98.03	98.03	99.22	99.23	100.22	100.1
Si	0.001	0.001	0.001	0.008	0.061	0.025	0.031
Ti	0.001	0.001	0.001	0.003	0.015	0.004	0.004
Al	1.677	1.664	1.667	0.006	0.009	0.004	0.006
Cr	0.319	0.330	0.316	0.217	0.276	0.114	0.135
Fe^{3+}	0.001	0.004	0.014	1.756	1.569	1.831	1.795
Fe^{2+}	0.251	0.261	0.241	0.945	0.884	0.937	0.930
Mn	0.002	0.003	0.003	0.035	0.057	0.019	0.022
Ni	0.006	0.006	0.007	0.004	0.009	0.003	0.005
Zn	0.000	0.000	0.000	0.000	0.000	0.000	0.000
Mg	0.741	0.729	0.751	0.026	0.112	0.056	0.059
Ca	0.000	0.000	0.000	0.002	0.002	0.002	0.008
Na	0.001	0.001	0.001	0.000	0.007	0.007	0.006
K	0.000	0.000	0.000	0.000	0.000	0.000	0.000
$Fe^{3+}/(Al + Cr + Fe^{3+})$	0.001	0.002	0.007	0.887	0.847	0.940	0.927
Cr#	0.160	0.165	0.159	0.974	0.969	0.966	0.959

strike-slip tectonics in the arc massif. The interpretation of the major erosional event documented by the Bāqoroq Formation is fundamental for the reconstruction of the evolution of Central Iran. Based on present distribution of rock outcrops in Central Iran, we note that lithologies of the metamorphic rocks exposed south of Nakhlak are compatible with features of metamorphic detritus supplied to the Bāqoroq Formation. If the source of metamorphic detritus in the Bāqoroq Formation is, indeed, the Anarak complex, it may be envisaged as: (a) a young metamorphic complex newly produced by Early–Middle Triassic collision tectonics; or (b) an older metamorphic basement involved in a new orogenic cycle. The new geochronological ages and reconstruction obtained by Bagheri & Stampfli (2008) indicate that a 'Variscan' event is recorded between the Great Kavir and the Biababak faults, and that a Permo-Triassic accretionary wedge was active in the Anarak region to the south of Nakhlak.

The occurrence of high-pressure mineralogical assemblages in the Chāh Gorbeh unit, already described in the literature (Sharkovski *et al.* 1984) but successively ignored by several authors (Davoudzadeh & Weber-Diefenbach 1987; Soffel *et al.* 1996; Alavi *et al.* 1997), is demonstrated by our analysis, constraining the P–T evolution of the Chāh Gorbeh unit to a subduction-related margin (Fig. 13). A minimum age for the high-pressure metamorphism is given by Ar–Ar stilpnomelane (233 ± 2 Ma), post-dating the event (Bagheri & Stampfli 2008), although younger ages have been published.

The exposure and unroofing of the accretionary wedge is recorded by the thick alluvial fans of the Ladinian Bāqoroq Formation and by the Doshākh and Bayazeh Flysch (Bagheri & Stampfli 2008), which also contain upper Ladinian–middle Carnian conodont faunas.

The Bāqoroq Formation is rich in clasts of marble and metapelitic rocks, very similar to the

Table 4. *Mineral chemistry of clinopyroxenes contained in the ultramafics of the Anarak Metamorphic Complex. Location of samples CI5 and CI6 is given in Figure 3*

Sample	CI5	CI5	CI5	CI6	CI6	CI5	CI5	CI5
Phase	cpx	cpx	cpx	cpx	cpx	ol	ol	ol
SiO_2	54.45	54.11	54.85	55.05	54.74	41.12	41.34	41.09
TiO_2	0	0.01	0.01	0.05	0.01	0	0	0
Al_2O_3	0.02	0.03	0.03	0.04	0.13	0	0.01	0
Cr_2O_3	0.07	0.05	0	0.01	0.01	0.04	0.03	0.05
FeO*	1.13	0.99	0.85	1.01	1.02	6.14	6.09	6.32
MnO	0.14	0.13	0.09	0.08	0.07	0.19	0.23	0.21
NiO	0.01	0	0.05	0.05	0.02	0.09	0.07	0.11
MgO	17.39	17.24	17.39	17.51	17.63	52.57	52.51	51.88
CaO	25.58	25.63	25.81	25.68	25.67	0.05	0.04	0.04
Na_2O	0.05	0.02	0.03	0.04	0.05	0	0.01	0.01
K_2O	0.01	0.01	0	0.01	0	0	0	0.01
Total	98.89	98.22	99.12	99.49	99.18	100.2	100.33	99.72
Si	1.998	1.998	2.004	2.003	1.998	0.987	0.992	0.993
Ti	0.000	0.000	0.000	0.001	0.000	0.000	0.000	0.000
Al	0.001	0.001	0.001	0.002	0.006	0.000	0.000	0.000
Cr	0.002	0.002	0.000	0.000	0.000	0.001	0.001	0.001
Fe^{3+}	0.001	0.000	0.001	0.004	0.000	0.000	0.000	0.000
Fe^{2+}	0.035	0.031	0.025	0.025	0.026	0.123	0.122	0.128
Mn	0.004	0.004	0.003	0.003	0.002	0.004	0.005	0.004
Ni	0.000	0.000	0.002	0.002	0.001	0.002	0.001	0.002
Mg	0.951	0.949	0.947	0.950	0.959	1.882	1.878	1.870
Ca	1.006	1.014	1.010	1.001	1.004	0.001	0.001	0.001
Na	0.004	0.001	0.002	0.003	0.004	0.000	0.001	0.001
K	0.001	0.001	0.000	0.001	0.000	0.000	0.000	0.000
X_{Mg}	0.965	0.969	0.975	0.974	0.974	0.935	0.935	0.932
Cation	4.002	4.001	3.995	3.994	4.000	3.000	3.000	3.000

metasedimentary units of the Morghāb schists and Palhāvand gneiss dated as Carboniferous. Uplift and erosion of the prism may be explained by the introduction of rigid bodies into the trench, as suggested by Bagheri & Stampfli (2008), who interpret a large part of the AMC as partially subducted seamounts.

The youngest Triassic unit of the Nakhlak succession, the Ashin Formation, is rich in felsic volcaniclastic turbiditic sandstones indicating a reprisal of the arc activity in the Late Ladinian–?Carnian. This might be ascribed to a transtensional stage of renewed subsidence and volcanism in an arc–trench setting associated with oblique convergence. The persistence of distinct and unmixed metamorphic and volcanic provenances during deposition of the Ashin Formation is thus explained by renewed volcanic activity in the north and continuing erosion of the accretionary prism in the south.

These data point to the occurrence of a collision event between an active margin and the Yazd block, although its precise age has not yet been defined so far. Conversely, the Late Carboniferous radiometric dates obtained in the Jandaq and Anarak region by Bagheri & Stampfli (2008) pose several questions as to their interpretation: no clear relationships between deformational structures, mineral assemblages and their pressure–temperature–time (P–T–t) evolution has been established by the authors. This implies that their radiometric data may be mixed ages not directly relatable to single metamorphic events. In addition, the occurrence of sillimanite–K-feldspar gneisses of the Jandaq belt, together with blueschists within the Variscan accretionary wedge complex, is fairly uncommon and needs more investigation, as these peculiar high-temperature metamorphic rocks can be more easily found in different geodynamic settings. Late Palaeozoic metamorphic rocks dated to the same time interval in the Talesh Mountains (Zanchetta *et al.* 2009) and in Afghanistan (Boulin 1988, 1991) generally show, in fact, a high-pressure imprint of blueschist–eclogitic conditions.

The occurrence of the Variscan–Eo-Cimmerian wedge within central Iran has been explained by the displacement of a large fragment of the Palaeotethys suture once located between Mashhad and

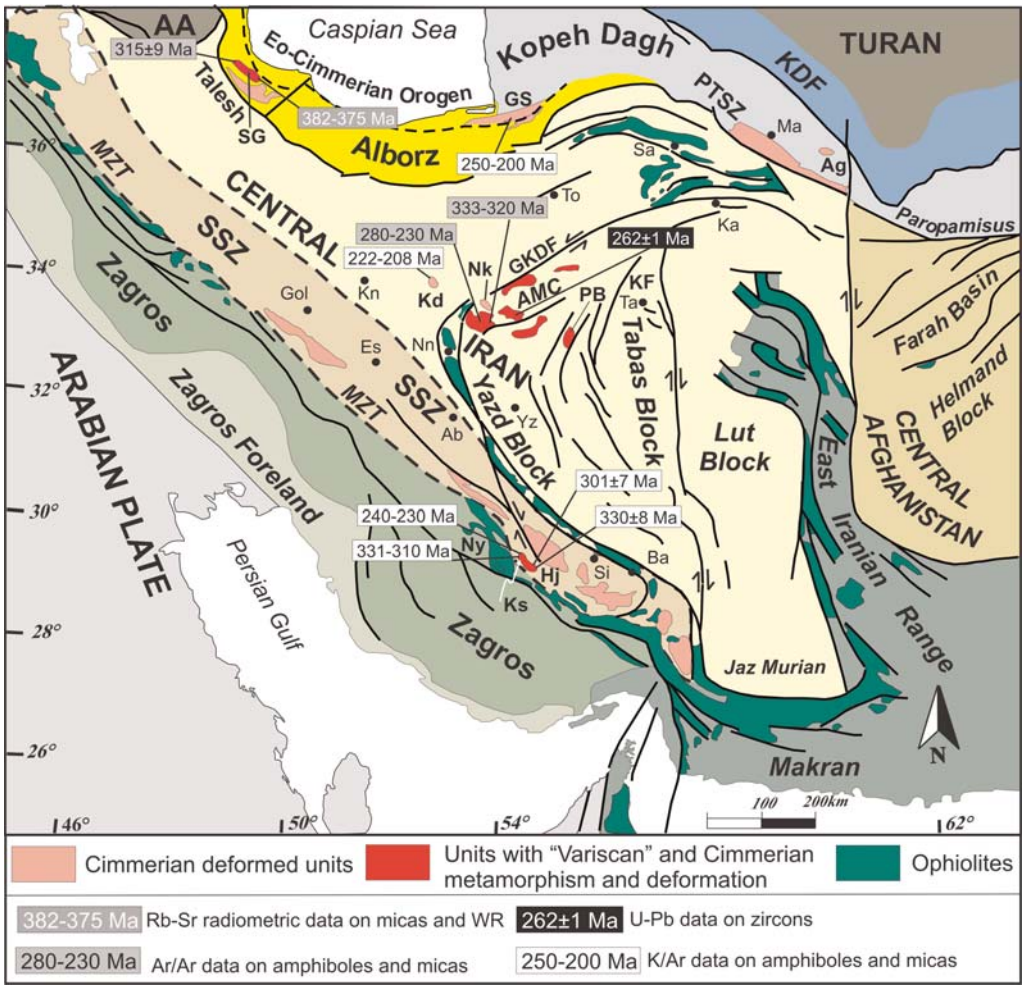

Fig. 13. Tectonic scheme of Iran with the main tectonic subdivisions, modified from the Geological Survey of Iran (1989). The location of the Eo-Cimmerian and Variscan units is highlighted. Green, Mesozoic ophiolites along the Main Zagros Thrust and other sutures. AA, Araxian–Azarbaijanian zone; Ab, Abadeh; Ag, Aghdarband Basin; AMC, Anarak Metamorphic Complex; Ba, Baft; Es, Esfahan; GKDF, Great Kavir–Doruneh fault system; Gol, Golpayegan; GS, Gorgan Schist; Ka, Kashmar; Kd, Ko-e-Dom; KDF, Kopeh Dagh Foredeep; KF, Kalmard Fault; Kn, Kashan; Ks, Kor-e-Sefid metamorphic complex; Hj, Hajiabad Metamorphic Complex; Ma, Mashhad; MZT, Main Zagros Thrust; Nk, Nakhlak Basin; Nn, Nain; Ny, Neyriz ophiolites; PB, Posht-e Badam; PTSZ, Palaeotethys Suture Zone; Sa, Sabzevar; SG, Shanderman and Gasht metamorphic complexes; Si, Sirjan; SSZ, Sanandaj–Sirjan Zone; Ta, Tabas; To, Torud; Yz, Yazd. Radiometric ages from the literature are reported for Variscan and Cimmerian metamorphosed units; see the text for references. WR, whole rock.

Afghanistan along the southern margin of the Turan domain (Bagheri & Stampfli 2008). According to their interpretation, the Late Cretaceous opening of the Nain–Sabzevar Ocean in a back-arc position was a consequence of the Neotethys subduction below the Sanandaj–Sirjan Zone. It separated parts of the accretionary complex from the Turan domain, and these portions were successively transported within Central Iran during the closure of the basin.

That interpretation follows from the idea, already proposed by several authors, that large counter-clockwise rotation (135°) of the whole Central Iran Microplate accompanied these processes (Wensink 1979; Davoudzadeh *et al.* 1981; Davoudzadeh & Weber-Diefenbach 1987; Soffel *et al.* 1996). However, several inconsistencies derive from the mechanisms of emplacement of the Jandak–Anarak terranes and especially the

supposed counter-clockwise rotations of the whole Central Iran region south of the Great Kavir–Doruneh fault system. New palaeomagnetic results and several geological data collected so far strongly question the amount of rotation postulated by most authors. Palaeomagnetic data (Muttoni *et al.* 2009) advise caution with regard to the hypothesis of Soffel *et al.* (1996) that a 135° counter-clockwise block rotation has occurred between the internal part of Central Iran and Europe since the Middle Triassic, an hypothesis that is based on sparse data from the Triassic sequence of Nakhlak. Multiple remagnetization events pervasively overprinted the volcaniclastic sandstones and siltstones at Nakhlak, whereas magnetization components of presumed primary age were observed only in a single nodular limestone interval. These primary components, when compared with reference European directions, suggest an Eurasian affinity, and no significant vertical axis rotations of the Nakhlak structure since the late Early Triassic (site IR04 in Muttoni *et al.* 2009). Undoubtedly, more data are required to unravel in detail the complex tectonic history of Iran, but we stress that our new palaeomagnetic data do not confirm a 135° counter-clockwise rotation of the internal part of Central Iran with respect to Eurasia since the Middle Triassic (Soffel *et al.* 1996). Similar conclusions were reached also by Besse *et al.* (1998).

A further geological argument against a large counter-clockwise vertical axis rotation of Central Iran is given by Wendt *et al.* (2005), who conclude that regional facies analysis of Upper Silurian–Lower Carboniferous successions is not consistent with a large 135° anticlockwise rotation of central Iran. Similarly, the present distribution of the units within the Anarak area indicates that a considerable rotation of the interior of Central Iran never occurred. In fact, the orientation of the three main Eo-Cimmerian elements in the area: the arc region of Nakhlak, the accretionary wedge, and the foreland area of the Yazd block, is consistent with their original palaeogeography in an arc–trench system.

The northern boundary of the Variscan units of Central Iran also poses several questions worthy of discussion. Bagheri & Stampfli (2008) recognized that the Variscan wedge is juxtaposed against the Airekan terrane south of the Doruneh fault south of Sabzevar, and that it consists of deformed peraluminous Cambrian granitic rocks with a U–Pb zircon age of 549 $\pm$ 15 Ma. These granitic rocks match the radiometric ages of other granitic intrusions forming the Gondwanan basement of Central Iran, such as near Posht-e-Badam (Ramezani & Tucker 2003) and the gneissic granites (Hassanzadeh *et al.* 2008) of the Shotori Kuh, 50 km NE of Torud on the north side of the Great Kavir Fault. In spite of this strong affinity, Bagheri & Stampfli (2008) hypothesize that the Airekan terrane is part of the Hun block, which detached during the Lower Palaeozoic from Gondwana and accreted to Eurasia before Variscan times. This interpretation is inconsistent with available information (Garzanti & Gaetani 2002; Natal'in & Sengör 2005 and references therein), as the so-called 'Turan domain', from which the Airekan terrane may derive, includes high-grade metamorphic rocks with a strong Late Palaeozoic metamorphic imprint.

Several authors have noted a strong affinity between the arc-related successions of the Aghdarband Triassic basin (Ruttner 1991, 1993) on the southern margin of Eurasia, east of Mashhad, and those of Nakhlak (Alavi *et al.* 1997). This supposed correlation has been used as the most persuasive argument to state that these localities were part of the same Palaeotethyan convergent margin, and that the Nakhlak succession was originally close to Aghdarband in the same trench–slope interval (Alavi *et al.* 1997). Balini *et al.* (2009) question the possible proximity of the two localities based on comparison among ammonoid faunas. Olenekian ammonoids from Aghdarband show a Periscaspian afinity, whereas the ones from Nakhlak show a typical Tethyan affinity: such an important palaeobiogeographic difference is not consistent with a proximity of the two areas.

Conclusions

We interpret the Triassic history of the Nakhlak–Anarak region as the result of the evolution of an arc–trench system related to Eo-Cimmerian orogenic events. The Triassic volcaniclastic successions of Nakhlak records the evolution of a volcanic arc facing an accretionary wedge, the remnants of which can be identified in the blueschists, ultramafic rocks and metacarbonates of the Anarak Metamorphic Complex (AMC). Deformation of the Nakhlak succession is presumably related to the collision of the arc–trench system with the Yazd block possibly during Late Triassic times, or to the subsequent Neo-Cimmerian event that strongly affected Central Iran between the end of the Jurassic and the beginning of the Cretaceous.

Intensive compressional phenomena affected the study area during the Tertiary, evidenced in folding and thrusting of the Eocene–Oligocene terrigenous successions in the Anarak region and in north-vergent reverse faults dismembering the AMC. Considerable strike-slip movements occurred along a major N–S-trending dextral strike-slip fault that displaced the eastern portion of the Nakhlak area.

This structure is part of the fault system that has affected Central Iran since the late Tertiary (Walker & Jackson 2004), causing differential block rotations along vertical axes.

New palaeomagnetic data obtained in the Triassic succession of Nakhlak indicate that there is no clear evidence of significant counter-clockwise rotations, and that palaeomagnetic information should be interpreted with extreme caution because of recent overprint affecting the succession. In any such case the latitude implied by the palaeomagnetic data suggests an Eurasian position for Nakhlak at the beginning of the Triassic.

Several contradictory and as-yet unresolved aspects of the Late Palaeozoic–Triassic evolution of Iran have been discussed in this paper, based on our field data and the analysis of the literature. Although several lines of evidence may suggest that large displacements of entire crustal blocks occurred during the amalgamation of Iran, the exact times, mechanism and the supposed amount of displacements of these terranes are still obscure. The interpretation of the Palaeozoic–Triassic evolution of Iran is also related to the understanding of the significance of the Variscan and Eo-Cimmerian metamorphism elsewhere in Iran, presently at large distances from the southern part of the Sanandaj–Sirjan Zone and its coeval metamorphic belts of Central and North Iran. Unravelling the palaeogeographical and structural relationships among these different crustal blocks is a difficult challenge for future geological research, and possibly represent a Mesozoic equivalent of the present-day 'Indonesian-type' orogenic scenario.

This work was funded by the MEBE programme (Proposal 3.30: 'Tectonic evolution of the Yazd, Tabas and Lut blocks (Central Iran) by means of palaeomagnetic, structural and stratigraphic data'; leader M. Mattei) in close collaboration with the Geological Survey of Iran. Dr M. R. Ghasemi, Dr A. Saidi and his colleagues of Geological Survey of Iran of Teheran are warmly thanked for continuous help and assistance in the field. The manuscript benefited from the reviews by A. Baud, M. Berberian and B. Natal'in. The three editors of the special volume, M.-F. Brunet, J. Granath and M. Wilmsen, are warmly thanked for their suggestions and accurate final revision of the manuscript.

Appendix

Quantitative mineral analyses were obtained with a JEOL 8200 Superprobe equipped with WDS spectrometers at the University of Milano. Operating conditions were 15 kV and 15 nA. Natural silicates were used as standards and the resulting data were corrected through a ZAF correction procedure.

Mineral formulae of amphibole from the blueschists of the Chāh Gorbeh unit were recalculated on the basis of 23 oxygens and 15 cation + K. Plagioclase formulae were recalculated on the basis of 8 oxygens per formula unit. White micas formulae result from considering all Fe as Fe^{2+} on the basis of 11 O. Cations in titanites were obtained on the basis of 3 total cations and 10 charges minus OH groups. Chlorites formulae were calculated on the basis of 28 oxygens. Olivine analyses were calculated considering all Fe as Fe^{2+} and cations sum equal to 3. Spinel formulae are expressed considering 3 cations and 8 charges. Clinopyroxenes analyses were recalculated on the basis of 6 oxygens and considering Fe^{3+} = Acmite.

References

ALAVI, M. 1991. Sedimentary and structural characteristics of the Paleo-Tethys remnants in northeastern Iran. *Geological Society of American Bulletin*, **103**, 983–992.

ALAVI, M. 1996. Tectonostratigraphic synthesis and structural style of the Alborz Mountain System in Iran. *Journal of Geodynamics*, **21**(1), 1–33.

ALAVI, M., VAZIRI, H., SEYED-EMAMI, K. & LASEMI, Y. 1997. The Triassic and associated rocks of the Nakhlak and Aghdarband areas in central and northeastern Iran as remnants of the southern Turanian active continental margin. *Geological Society of America Bulletin*, **109**, 1563–1575.

ALLEN, M. B., GHASSEMI, M. R., SHAHRABI, M. & QORASHIB, M. 2003. Accommodation of late Cenozoic oblique shortening in the Alborz range, northern Iran. *Journal of Structural Geology*, **25**, 659–672.

ANGELIER, J. 1984. Tectonic analysis of fault slip data sets. *Journal of Geophysical Research*, **89**, 5835–5848.

ANGELIER, J. 1990. Inversion of field data in fault tectonics to obtain the regional stress – III. A new rapid direct inversion method by analytical means. *Geophysical Journal International*, **103**(1), 363–376.

ANGIOLINI, L., GAETANI, M., MUTTONI, G., STEPHENSON, M. H. & ZANCHI, A. 2007. Tethyan oceanic currents and climate gradients 300 m.y. ago. *Geology*, **35**, 1071–1074.

APTED, M. J. & LIOU, J. G. 1983. Phase relations among greenschists, epidote-amphibolite, and amphibolite in a basalt system. *American Journal of Science*, **283A**, 328–354.

BAGHERI, S. & STAMPFLI, G. M. 2008. The Anarak, Jandaq and Posht-e-Badam metamorphic complexes in central Iran: New geological data, relationships and tectonic implications. *Tectonophysics*, **451**, 123–155.

BALINI, M., NICORA, A. *ET AL.* 2009. The Triassic stratigraphic succession of Nakhlak (Central Iran), a record from an active margin. *In*: BRUNET, M.-F., WILMSEN, M. & GRANATH, J. W. (eds) *South Caspian to Central Iran Basins*. Geological Society, London, Special Publications, **312**, 287–321.

BERBERIAN, M. & KING, G. 1981. Toward a paleogeography and tectonic evolution of Iran. *Canadian Journal of Earth Science*, **18**, 210–265.

BERRA, F., ZANCHI, A., MATTEI, M. & NAWAB, A. 2007. Late Cretaceous transgression on a Cimmerian

high (Neka Valley, Eastern Alborz, Iran): A geodynamic event recorded by glauconitic sands. *Sedimentary Geology*, **199**, 189–204.

BESSE, J., TORCQ, F., GALLET, Y., RICOU, L.-E., KRYSTYN, L. & SAIDI, A. 1998. Late Permian to Late Triassic palaeomagnetic data from Iran: constraints on the migration of the Iranian bock through the Tethyan Ocean and initial destruction of Pangaea. *Geophysical Journal International*, **135**, 77–92.

BOULIN, J. 1988. Hercynian and Eocimmerian events in Afghanistan and adjoining regions. *Tectonophysics*, **148**, 253–278.

BOULIN, J. 1991. Structures in Southwest Asia and evolution of the eastern Tethys. *Tectonophysics*, **196**, 211–268.

BRUNET, M.-F., KOROTAEV, M. V., ERSHOV, A. V. & NIKISHIN, A. M. 2003. The South Caspian Basin: a review of its evolution from subsidence modelling. *Sedimentary Geology*, **156**, 119–148.

CRAWFORD, M. A. 1977. A summary of isotopic age data for Iran, Pakistan and India. *In*: *Livre a la mémoire de A. F. de Lapparent*. Societé Géologique de France, Mémoire, **8**, 251–260.

DAVIDOF, V. I. & AREFIFARD, A. 2007. Tectonics and paleogeographic applications of Peri-Gondwanan Permian Fusulinid Fauna from Kalmard region, East-Central Iran. *Permophiles*, **49**, 13–24.

DAVOUDZADEH, M. & WEBER-DIEFENBACH, K. 1987. Contribution to the paelogeography, stratigraphy and tectonics of the Upper Paleozoic in Iran. *Neues Jahrbuch für Geologie und Paläontologie, Abhandlungen*, **175**(2), 121–146.

DAVOUDZADEH, M., SOFFEL, H. & SCHMIDT, K. 1981. On the rotation of Central-East-Iran microplate. *Neues Jahrbuch für Geologie und Paläontologie, Monatshefte*, **3**, 180–192.

DERCOURT, J., GAETANI, M. *ET AL*. 2000. *Atlas Peri-Tethys. Palaeogeographical Maps* (24 maps and explanatory notes I –XX). CCGM/CGMW, Paris.

DICK, H. J. B. & BULLEN, T. 1984. Chromian spinel as a petrogenetic indicator in abyssal and alpine-type peridotites and spatially associated lavas. *Contribution to Mineralogy and Petrology*, **86**, 54–76.

DICKINSON, W. R. 1985. Interpreting provenance relations from detrital modes of sandstones. *In*: ZUFFA, G. G. (ed.) *Provenance of Arenites*. NATO ASI Series, **148**, 333–361.

FÜRSICH, F. T., WILMSEN, M.,, SEYED-EMAMI, K. & MAJIDIFARD, M. R. 2009. Lithostratigraphy of the Upper Triassic–Middle Jurassic Shemshak Group of Northern Iran. *In*: BRUNET, M.-F., WILMSEN, M. & GRANATH, J. W. (eds) *South Caspian to Central Iran Basins*. Geological Society, London, Special Publications, **312**, 129–160.

GAETANI, M., ANGIOLINI, L. *ET AL*. 2009. Pennsylvanian–Early Triassic stratigraphy in the Alborz Mountains (Iran). *In*: BRUNET, M.-F., WILMSEN, M. & GRANATH, J. W. (eds) *South Caspian to Central Iran Basins*. Geological Society, London, Special Publications, **312**, 79–128.

GARZANTI, E., DOGLIONI, C., VEZZOLI, G. & ANDÒ, S. 2007. Orogenic belts and orogenic sediment provenance. *Journal of Geology*, **115**, 315–334.

GARZANTI, E. & GAETANI, M. 2002. Unroofing history of Late Palaeozoic magmatic arcs within the 'Turan Plate' (Tuarkyr, Turkmenistan). *Sedimentary Geology*, **151**, 67–87.

GARZANTI, E. & VEZZOLI, G. 2003. A classification of metamorphic grains in sands based on their composition and grade. *Journal of Sedimentary Research*, **73**, 830–837.

GHASEMI, H., JUTEAU, T., BELLON, H., SABZEHEI, M., WHITECHURCH, H. & RICOU, L.-E. 2002. The mafic–ultramafic complex of Sikhoran (central Iran): a polygenetic ophiolite complex. *Comptes Rendus Geoscience*, **334**, 431–438.

GHASEMI, A. & TALBOT, C. J. 2006. A new tectonic scenario for the Sanandaj–Sirjan Zone (Iran). *Journal of Asian Earth Sciences*, **26**, 683–693.

GEOLOGICAL SURVEY OF IRAN. 1972. *Yazd*, scale 1:250 000. Geological Survey of Iran, Tehran.

GEOLOGICAL SURVEY OF IRAN. 1976. *Torud*, scale 1:25 000. Geological Survey of Iran, Tehran.

GEOLOGICAL SURVEY OF IRAN. 1977. *Ferdows*, scale 1:250 000. Geological Survey of Iran, Tehran.

GEOLOGICAL SURVEY OF IRAN. 1984*a*. *Anarak*, scale 1:100 000. Geological Survey of Iran, Tehran.

GEOLOGICAL SURVEY OF IRAN. 1984*b*. *Anarak*, scale 1:250 000. Geological Survey of Iran, Tehran.

GEOLOGICAL SURVEY OF IRAN. 1984*c*. *Khur*, scale 1:250 000. Geological Survey of Iran, Tehran.

GEOLOGICAL SURVEY OF IRAN. 1987. *Jandaq*, scale 1:250 000. Geological Survey of Iran, Tehran.

GEOLOGICAL SURVEY OF IRAN. 1989. *Geological Map of Iran*, scale 1:2 500 000. Geological Survey of Iran, Tehran.

GEOLOGICAL SURVEY OF IRAN. 1993. *Sikhoran*, scale 1:250 000. Geological Survey of Iran, Tehran.

GEOLOGICAL SURVEY OF IRAN. 2003. *Nakhlak*, scale 1:100 000. Geological Survey of Iran, Tehran.

GOLONKA, J. 2004. Plate tectonic evolution of the southern margin of Eurasia in the Mesozoic and Cenozoic. *Tectonophysics*, **381**, 235–273.

GUIRAUD, M., HOLLAND, T. J. B. & POWELL, R. 1990. Calculated mineral equilibria in the greenschist–blueschist–eclogite facies in Na_2O–FeO–MgO–Al_2O_3–SiO_2–H_2O: methods, results and geological applications. *Contributions to Mineralogy and Petrology*, **104**, 85–98.

HASSANZADEH, J., STOCKLI, D. F. *ET AL*. 2008. U–Pb zircon geochronology of late Neoproterozoic–Early Cambrian granitoids in Iran: Implications for paleogeography, magmatism, and exhumation history of Iranian basement. *Tectonophysics*, **451**, 71–96.

HOLZER, H. F. & GHAZEMIPOUR, R. 1969. Geology of the Nakhlak lead mine area (Anarak district, Central Iran). *Geological Survey of Iran, Report*, **21**, 7–26.

HORTON, B. K., HASSANZADEH, J. *ET AL*. 2008. Detrital zircon provenance of Neoproterozoic to Cenozoic deposits in Iran: Implications for chronostratigraphy and collisional tectonics. *Tectonophysics*, **451**, 97–122.

LEVEN, E. J. & GORGIJ, M. N. 2006. Upper Carboniferous–Permian stratigraphy and fusulinids from the Anarak region, Central Iran. *Russian Journal of Earth Sciences*, **8**, ES2002; doi:10.2205/2006ES000200.

MARSAGLIA, K. M. & INGERSOLL, R. V. 1992. Compositional trends in arc-related, deep-marine sand and sandstone: a reassessment of magmatic-arc provenance. *Geological Society American Bulletin*, **104**, 1637–1649.

MOHAJJEL, M. & FERGUSSON, C. L. 2000. Dextral transpression in Late Cretaceous continental collision, Sanandaj–Sirjan Zone, western Iran. *Journal of Structural Geology*, **22**, 1125–1139.

MUTTONI, G., MATTEI, M., BALINI, M., ZANCHI, A., GAETANI, M. & BERRA, F. 2009. The drift history of Iran from the Ordovician to the Triassic. *In*: BRUNET, M.-F., WILMSEN, M. & GRANATH, J. W. (eds) *South Caspian to Central Iran Basins*. Geological Society, London, Special Publications, **312**, 7–29.

NATAL'IN, B. A. & SENGÖR, A. M. S. 2005. Late Palaeozoic to Triassic evolution of the Turan and Scythian platforms: The pre-history of the Palaeo-Tethyan closure. *Tectonophysics*, **404**, 175–202.

RACHIDNEJAD-OMRANI, N., HACHEM EMAMIB, M., SABZEHEI, M., RASTAD, E., BELLON, H. & PIQUÉ, A. 2002. Lithostratigraphie et histoire paléozoïque à paléocène des complexes métamorphiques de la région de Muteh, zone de Sanandaj–Sirjan (Iran méridional). *Comptes Rendus Geoscience*, **334**, 1185–1191.

RAMEZANI, J. & TUCKER, R. 2003. The Saghand region, Central Iran: U–Pb geochronology, petrogenesis and implications for Gondwana tectonics. *American Journal of Science*, **303**, 622–665.

REYRE, D. & MOHAFEZ, S. 1970. Une première contribution des accords NIOC-ERAP à la connaissance géologique de l'Iran. *Revue de l'Institut Français du Pétrole*, **25**, 687–713, 979–1014.

RUTTNER, A. W. 1991. *Geology of Aqdarband Area (Kopeh Dagh, NE-Iran); With a Geological Map 1:12 500. The Triassic of Aqdarband (AqDarband), NE-Iran, and its Pre-Triassic Frame.* Abhandlungen der Geologischen Bundesanstalt Wien, **38**.

RUTTNER, A. W. 1993. Southern borderland of Triassic Laurasia in north-east Iran. *Geologische Rundschau*, **82**, 110–120.

SAIDI, A., BRUNET, M.-F. & RICOU, L.-E. 1997. Continental accretion of the Iran Block to Eurasia as seen from Late Palaeozoic to early Cretaceous subsidence curves. *Geodinamica Acta*, **10**, 189–208.

SENGÖR, A. M. C. 1979. Mid-Mesozoic closure of Permo-Triassic Tethys and its implications. *Nature*, **279**, 590–593.

SENGÖR, A. M. C. 1990. A new model for the late Palaeozoic-Mesozoic tectonic evolution of Iran and implications for Oman. *In*: ROBERTSON, A. H., SEARLE, M. P. & RIES, A. C. (eds) *The Geology and Tectonics of the Oman region*. Geological Society, London, Special Publications, **49**, 797–831.

SEYED-EMAMI, K. 2003. Triassic in Iran. *Facies*, **48**, 95–106.

SHARKOVSKI, M., SUSOV, M. & KRIVYAKIN, B. 1984. *Geology of the Anarak area (Central Iran). Explanatory Text of the Anarak Quadrangle Map 1:250 000*. Geological Survey of Iran, V/O 'Tecnoexport' USSR Ministry of Geology, Reports, **19**.

SHEIKHOLESLAMI, R., BELLON, H., EMAMI, H., SABZEHEI, M. & PIQUÉ, A. 2003. Nouvelles données structurales et datations $^{40}K-^{40}Ar$ sur les roches métamorphiques de la région de Neyriz (zone de Sanandaj–Sirjan, Iran méridional). Leur intérêt dans le cadre du domaine néo-téthysien du Moyen-Orient. *Comptes Rendus Geoscience*, **335**, 981–991.

SOFFEL, H., DAVOUDZADEH, M., ROLF, C. & SCHMIDT, S. 1996. New paleomagnetic data from Central Iran and a Triassic paleoreconstruction. *Geologische Rundschau*, **85**, 293–302.

STAMPFLI, G. M. & BOREL, G. D. 2002. A plate tectonic model for the Palaeozoic and Mesozoic constrained by dynamic plate boundaries and restored synthetic oceanic isochrones. *Earth Planetary Sciences Letters*, **196**, 17–33.

STAMPFLI, G. M., MARCOUX, J. & BAUD, A. 1991. Tethyan margins in space and time. *Palaeogeography, Palaeoclimatology, Palaeoecology*, **87**, 373–409.

STÖCKLIN, J. 1974. Possible ancient continental margins in Iran. *In*: BURK, C. A. & DRAKE, C. L. (eds) *The Geology of Continental Margins*. Springer, Berlin, 873–887.

TORSVIK, T. H. & COCKS, R. M. 2004. Earth geography from 400 to 250 Ma: a palaeomagnetic, faunal and facies review. *Journal of the Geological Society, London*, **161**, 555–572.

WALKER, R. & JACKSON, J. 2004. Active tectonics and late Cenozoic strain distribution in central and eastern Iran. *Tectonics*, **23**, TC5010; doi:10.1029/2003TC001529.

WENDT, J., KAUFMANN, B., BELKA, Z., FARSAN, N. & BAVANDPUR, A. K. 2002. Devonian/Lower Carboniferous stratigraphy, facies patterns and palaeogeography of Iran. Part I. Southeastern Iran. *Acta Geologica Polonica*, **52**(2), 129–168.

WENDT, J., KAUFMANN, B., BELKA, Z., FARSAN, N. & BAVANDPUR, A. K. 2005. Devonian/Lower Carboniferous stratigraphy, facies patterns and palaeogeography of Iran Part II. Northern and Central Iran. *Acta Geologica Polonica*, **55**(1), 31–97.

WENSINK, H. 1979. The implications of some palaeomagnetic data from Iran from its structural history. *Geologie en Mijnbow*, **58**, 175–185.

WOODCOCK, N. H. & SCHUBERT, C. 1995. Continental strike-slip tectonics. *In*: HANCOCK, P. L. (ed.) *Continental Deformation*. Pergamon, Oxford, 251–263.

ZANCHETTA, S., ZANCHI, A., VILLA, I., POLI, S. & MUTTONI, G. 2009. The Shanderman eclogites: a Late Carboniferous high-pressive event in the NW Talesh Mountains (NW Iran). *In*: BRUNET, M.-F., WILMSEN, M. & GRANATH, J. W. (eds) *South Caspian to Central Iran Basins*. Geological Society, London, Special Publications, **312**, 57–78.

ZANCHI, A., BERRA, F., MATTEI, M., GHASSEMI, M. & SABOURI, J. 2006. Inversion tectonics in Central Alborz, Iran. *Journal of Structural Geology*, **28**, 2023–2037.

ZANCHI, A., ZANCHETTA, S. *ET AL.* 2009. The Eo-Cimmerian (Late? Triassic) orogeny in North Iran. *In*: BRUNET, M.-F., WILMSEN, M. & GRANATH, J. W. (eds) *South Caspian to Central Iran Basins*. Geological Society, London, Special Publications, **312**, 31–55.